RESPONSE OF AN ELASTIC HALF-SPACE TO FINITE SIZED SOURCES

by

Abdülkadir Başakar

Submitted to the Faculty of Engineering

in Partial Fulfillment of

the Requirements for the Degree of

MASTER OF SCIENCE

in

MECHANICAL ENGINEERING

Boğaziçi University

1982

This thesis has been approved by

Dr. Ahmet CERANOĞLU
(Thesis Supervisor)


Prof.Dr. Akın TEZEL

Doç.Dr. Başar CİVELEK

ABSTRACT

Analysis of the transient response of an isotropic, homogeneous and elastic half-space due to the application of a point, a finite line, and areal sources are presented in this thesis. The source is either buried or on the surface while the receiver is always taken on the surface. Solutions are obtained for vertically and radially oriented sources and for different values of z_o depth of the source and r_o radial distance from the source to the receiver. The response due to finite sized line and areal sources are obtained by integrating numerically the point source results along the line and over the area respectively.

The results obtained in this work can be used to explain the effect of the size of the transducers used in Nondestructive Testing of materials. Here, the solution gives the response of a half-space for a Heaviside's step input function.

In the numerical calculations, using the generalized ray theory, the response of the half-space is expressed in terms of the contributions from individual rays. Each ray is expressed in terms of integrals in the complex Laplace transform space, and the Cagniard's method is used to take the inverse transform of the expressions. As each ray has a distinct path and a certain arrival time, only the rays that arrive prior to the time of interest are considered.
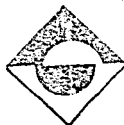
ÖZETÇE

Bu tezde, bir nokta kuvvet, bir sonlu çizgi kuvvet ve bir yüzeysel kuvvet etkisindeki homojen, elastik ve isotropik bir yarı uzayın zamana bağlı tepkisi incelenmiştir. Kuvvet yarı uzayın içinde ya da üzerinde, alıcı ise daima üzerinde bulunmaktadır. Kuvvetler dikey ya da yatay olarak çeşitli derinlik z_0 ve yatay uzaklıklarda r_0 uygulanarak çözümler elde edilmiştir. Sonlu çizgi ve yüzeysel kuvvet uygulanması durumlarında çözümler, nokta kuvvet için bulunan çözümlerin nümerik olarak çizgi ya da yüzey üzerinde entegre edilmesi ile bulunmuştur.

Elde edilen sonuçlar, tahribatsız malzeme kontrollerinde kullanılan çevireçlerin (transducer) yüzey alanlarının kontrol üzerindeki etkisini saptamakta kullanılabilir. Burada çözümler yarı uzayda "Heaviside basamak" fonksiyonu için bulunmuştur.

Sayısal hesaplarda, genel dalga teorisi kullanılarak, yarı uzayın tepkisi, ayrı ayrı dalgalara oluşan tepkiler cinsinden ifade edilmiştir. Her dalganın hareketi complex Laplace dönüşüm uzayında integrallerle ifade edilmiş, ve ters dönüşümler Cagniard metodu kullanılarak elde edilmiştir. Dalgaların takip ettikleri yol ve varış zamanları farklı olduğundan, sadece, ilgilenilen zaman içinde alıcıya ulaşan dalgalar değerlendirmeye alınmıştır.

ACKNOWLEDGEMENT

TABLE OF CONTENTS

LIST OF FIGURES

Chapter I

INTRODUCTION

The quality and integrity of a material is greatly affected by the number and size of the defects such as cracks and voids contained in the material. Under loading and service conditions, these defects may cause failures. Hence, it is important to detect them before any failure occurs. The technology used to detect these defects is called the Nondestructive Testing of materials, and a widely used technique in this area is acoustic emission. To test a material, forces are applied on structure; and the transient elastic waves generated by the defects, due to the rapid release of energy at these points, that is acoustic emissions, are picked up by sensitive transducers placed on the structure. The recorded signals are used to find the location and the character of the defects.

To make an accurate evaluation of a material, the transducer to be used should be calibrated. The transducers are calibrated as a source and as a receiver, through a comparison with a standard source and a standard receiver respectively. For this purpose, a transducer of known characteristics such as a capacitive transducer and a transfer media of known theoretical solution is used. A large block representing a half-space can be chosen as the transfer media so that its theoretical solution can easily be obtained. In addition, it is important to know the effect of the size of the source and the receiver, namely, the transducer used in Nondestructive Testing of materials.

The purpose of this work is to study the response of a homogeneous isotropic and elastic half-space due to a finite sized line and areal forces. The basis for such forces is the single concentra-

ted force. That is, the response due to the finite sized sources
can be obtained by integrating numerically the single force results
over a finite line or area. Surface response of the half-space due
to buried and surface forces will be presented.

The method of generalized rays will be used in the mathematical
analysis of the problem. In this method, the response of the media
is decomposed into contributions from individual rays originating
at the source location and reaching the receiver after travelling
different paths. Since each ray has a definite arrival time, only
a finite number of them have to be calculated within a given time
of interest. The expressions for each ray are in terms of complicated
integrals in the complex Laplace transform space. The inverse Laplace
transform will be found using the modified Cagniard De Hoop method.

In Chapter II, the basic equations of elasticity are given,
and the particular solution for the displacements due to a single
force are found.

In Chapter III, a brief history of the method of generalized
rays is given. Also in this chapter, the reflection coefficients at
a free surface and the ray solution for a half-space are discussed.
The expressions for the source and receiver functions at different
locations are also presented at the end of this chapter.

In Chapter IV, application of the Cagniard's method and the
inversion of Laplace transform are discussed in detail.

Finally, in Chapter V, numerical results are presented for a
point, and a finite line and areal sources. Surface displacements
of a half-space are given for different locations of the aforemen-
tioned sources.

EQUATIONS OF ELASTICITY AND SOLUTION FOR

A POINT SOURCE IN AN UNBOUNDED MEDIUM

The basic equations of dynamic elasticity and the particular
solution for a single concentrated force in an unbounded, isotropic,
homogeneous and elastic medium will be presented in this chapter.
The linearized equations of motion and the solution of them for a
single force in an infinite media can be found in the classical book
by Love [14] and Achenbach [2]. Here, these solutions will be given
in terms of Laplace transforms so that one can modify them to the
half-space problems as well.

2.1. DYNAMIC EQUATIONS OF ELASTICITY

When forces are applied, a solid body deforms and the distance
between any two point changes. The ratio of the relative changes to
the original distances are called strains. In this work, as the strains
are considered to be small, the linear equations of the theory of
elasticity are used.

In the linear theory of elasticity, for a homogeneous, isotropic,
and elastic body, the displacement field, $\underset{\sim}{u}(\underset{\sim}{r},t)$, satisfies the
equation [2]

$$\mu\nabla^2\underset{\sim}{u} + (\lambda+2\mu)\underset{\sim}{\nabla}(\underset{\sim}{\nabla}\cdot\underset{\sim}{u}) + \rho\underset{\sim}{F} = \rho\ddot{\underset{\sim}{u}} \qquad (2.1)$$

where ρ is the mass density, λ and μ are the Lame constants of the
material, $\underset{\sim}{F}$ is the body force per unit mass and a "dot" denotes the
partial differentiation with respect to time, t. In the equation
above, ∇^2 is the usual Laplacian operator, and $\underset{\sim}{\nabla}\cdot$ and $\underset{\sim}{\nabla}$ are the

divergence and gradient operators respectively. For an isotropic elastic material, the stress-displacement relations are given by [2]

$$\underset{\sim}{\sigma} = \lambda(\nabla\cdot\underset{\sim}{u})\underset{\approx}{I} + 2\mu(\nabla\underset{\sim}{u} + \underset{\sim}{u}\nabla) \qquad\qquad (2.2)$$

where $\underset{\sim}{\sigma}$ and $\underset{\approx}{I}$ are the Cauchy stress and unit tensors respectively, and $\underset{\sim}{u}\nabla$ is the transpose of $\nabla\underset{\sim}{u}$.

Equations (2.1) and (2.2) must be satisfied at every interior point of a body occupying a volume V in space bounded by a surface S. In addition, the solution $\underset{\sim}{u}$ must satisfy certain boundary conditions on S and the initial conditions at $t=0$. The initial conditions are usually of the form

$$\underset{\sim}{u}(\underset{\sim}{r},0) = \underset{\sim}{u}_0(\underset{\sim}{r})$$

$$\qquad\qquad (2.3)$$

$$\underset{\sim}{\dot{u}}(\underset{\sim}{r},0) = \underset{\sim}{\dot{u}}_0(\underset{\sim}{r}) \ ,$$

while the boundary conditions can be in terms of displacements or tractions or both. The boundary conditions involving tractions only are specified as

$$\underset{\sim}{T} = \underset{\approx}{\sigma}\cdot\underset{\sim}{n} \qquad \text{on S} \qquad\qquad (2.4)$$

In an unbounded medium radiation conditions must be used instead of boundary conditions. That is, all components of the displacement vector must vanish at infinity.

Our approach to solve Eq.(2.1) will be first to reduce it to wave equations, using the Helmholtz decomposition theorem,

$$\underset{\sim}{u} = \nabla\phi + \nabla\times\underset{\sim}{\psi}_1 \quad , \qquad \nabla\cdot\underset{\sim}{\psi}_1 = 0$$

$$\text{(2.5)}$$

$$\underset{\sim}{F} = \nabla G + \nabla\times\underset{\sim}{H} \quad , \qquad \nabla\cdot\underset{\sim}{H} = 0$$

where the single valued vector fields, $\underset{\sim}{u}$ and $\underset{\sim}{F}$, are expressed in terms of the gradient of scalar fields, ϕ and G, and the curl of vector fields, $\underset{\sim}{\psi}_1$ and $\underset{\sim}{H}$, respectively. Substituting Eq.(2.5) into Eq.(2.1), one obtains the wave equations in terms of the potentials,

$$c^2\nabla^2\phi + G = \ddot{\phi} \quad , \quad c^2 = (\lambda+2\mu)/\rho$$

$$\text{(2.6)}$$

$$C^2\nabla^2\underset{\sim}{\psi}_1 + \underset{\sim}{H} = \ddot{\underset{\sim}{\psi}}_1 \qquad C^2 = \mu/\rho$$

The potentials ϕ and $\underset{\sim}{\psi}_1$ give rise to longitudinal waves (P-waves), travelling with a speed c, and shear waves (S-waves), travelling with a speed C, respectively. Equation (2.6) gives the complete solutions of Eq.(2.1), (Sternberg [23]). For plane waves the particle motion of a P-wave is in the direction of $\underset{\sim}{n}$, the normal to the wave front, and that of S-wave is in a plane perpendicular to $\underset{\sim}{n}$.

In curvilinear coordinate systems, the equations in terms of the vector potential are coupled, hence, it is difficult to obtain a solution. However, in the case of propagation of elastic waves, the particle displacement due to S-wave can be further decomposed into two orthogonal components; one that is parallel to a given direction is called the SH or horizontally polarized shear wave component while the other one perpendicular to it, is called the SV or vertically polarized shear wave component. In the case of waves in a half-space SH-waves are associated with displacements parallel to the surface.

Thus, a decomposition of the form

$$\underset{\sim}{\psi}_1 = \chi\underset{\sim}{e}_z + \nabla\times(\psi\underset{\sim}{e}_z) \qquad (2.7)$$

$$\underset{\sim}{H} = H_1\underset{\sim}{e}_z + \nabla\times(H_2\underset{\sim}{e}_z) \qquad (2.8)$$

is possible.

In these expressions, $\underset{\sim}{e}_z$ is a unit vector perpendicular to the surface of the half-space. Using the decomposition, Eq.(2.6) yields

$$c^2\nabla^2\phi + G = \ddot{\phi}$$

$$c^2\nabla^2\psi + H_2 = \ddot{\psi} \qquad (2.9)$$

$$c^2\nabla^2\chi + H_1 = \ddot{\chi}$$

and the initial conditions in terms these potentials will be in the form

$$\phi(\underset{\sim}{r},0) = \phi_0(\underset{\sim}{r}) \qquad , \qquad \dot{\phi}(\underset{\sim}{r},0) = \dot{\phi}_0(\underset{\sim}{r})$$

$$\psi(\underset{\sim}{r},0) = \psi_0(\underset{\sim}{r}) \qquad , \qquad \dot{\psi}(\underset{\sim}{r},0) = \dot{\psi}_0(\underset{\sim}{r}) \qquad (2.10)$$

$$\chi(\underset{\sim}{r},0) = \chi_0(\underset{\sim}{r}) \qquad , \qquad \dot{\chi}(\underset{\sim}{r},0) = \dot{\chi}_0(\underset{\sim}{r})$$

It is understood that ψ gives rise to SV-wave and χ to SH-wave.

In the analysis of waves in a half-space, we introduce the following non-dimensional quantities

$$\underset{\sim}{u} = r_o \underset{\sim}{\hat{u}} \quad , \quad t = r_o \hat{t}/c \quad , \quad \underset{\sim}{\nabla} = r_o^{-1} \underset{\sim}{\hat{\nabla}}$$

$$\phi = r_o^2 \hat{\phi} \quad , \quad \psi = r_o^3 \hat{\psi} \quad , \quad \chi = r_o^2 \hat{\chi}$$

$$G = c^2 \hat{G} \quad , \quad H_2 = r_o c^2 \hat{H}_2 \quad , \quad H_1 = c^2 \hat{H}_1 \tag{2.11}$$

$$\underset{\sim}{\sigma} = (\lambda + 2\mu) \underset{\sim}{\hat{\sigma}} \quad , \quad \kappa = c/C$$

where "^" shows the non-dimensional quantities and r_o is the radial distance between the source and the receiver. Using Eq.(2.11), Eq.(2.9) can be written in non-dimensional form

$$\hat{\nabla}^2 \hat{\phi} + \hat{G} = \ddot{\hat{\phi}}$$

$$\hat{\nabla}^2 \psi + \kappa^2 \hat{H}_2 = \kappa^2 \ddot{\psi} \tag{2.12}$$

$$\hat{\nabla}^2 \hat{\chi} + \kappa^2 \hat{H}_1 = \kappa^2 \ddot{\hat{\chi}}$$

The sign "^" will be dropped, as all the quantities in this thesis will be non-dimensional.

2.2 PARTICULAR SOLUTION FOR A SINGLE FORCE

In this section, the solutions for the potentials ϕ , ψ and χ will be obtained. For that purpose, Laplace transform of $f(\underset{\sim}{r},t)$, denoted as $\bar{f}(\underset{\sim}{r},s)$, is defined by

$$\bar{f}(\underset{\sim}{r},s) = \int_o^\infty f(\underset{\sim}{r},t)e^{-st}\, dt$$

<div align="right">(2.13)</div>

$$f(\underset{\sim}{r},t) = \frac{1}{2\pi i} \int_{Br} \bar{f}(\underset{\sim}{r},s)e^{st}\, ds$$

where s is the transform variable and Br in the second expression is the Bromwich contour in the complex s-plane, which is a line parallel to the imaginary axis and to the right of all singularities of $\bar{f}(\underset{\sim}{r},s)$. Note that, the second equation defines the inverse transform.

Consider a concentrated force with a time function f(t) applied at a point $(0,0,z_o)$ and acting in the direction of a unit vector $\underset{\sim}{a}$, (Fig.1). Vector $\underset{\sim}{a}$ is defined as
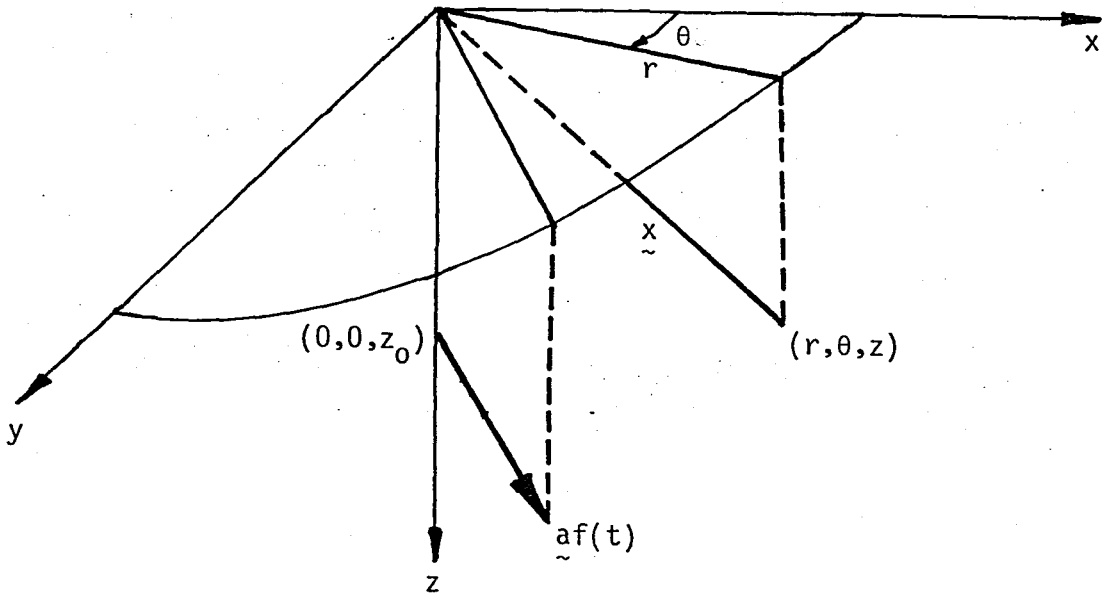
Figure 1. Geometry of an oblique, concentrated force.

$$\underset{\sim}{a} = a_1\underset{\sim}{e}_1 + a_2\underset{\sim}{e}_2 + a_3\underset{\sim}{e}_3$$

$$= a_r\underset{\sim}{e}_r + a_\theta\underset{\sim}{e}_\theta + a_z\underset{\sim}{e}_z$$

(2.14)

where $\underset{\sim}{e}_1$, $\underset{\sim}{e}_2$, $\underset{\sim}{e}_3$ and $\underset{\sim}{e}_r$, $\underset{\sim}{e}_\theta$, $\underset{\sim}{e}_z$ are the unit vectors in cartesian and cylindrical coordinates respectively. Components of the vector $\underset{\sim}{a}$ in the cylindrical coordinates are related to the components in cartesian coordinates through the relations

$$a_r = a_1\cos\theta + a_2\sin\theta$$

$$a_\theta = -a_1\sin\theta + a_2\cos\theta$$

(2.15)

$$a_z = a_3$$

Note that similar relations apply for the unit vectors. The concentrated force, $\underset{\sim}{F}$ is represented by

$$\underset{\sim}{F} = \underset{\sim}{a}F_0 f(t)\delta(z-z_0)\delta(r)/2\pi r$$

(2.16)

The particular solution of the potentials are (see Appendix A)

$$\bar{\phi}(\underset{\sim}{r},s;\underset{\sim}{a}) = a_z s^2\bar{F}(s) \int_0^\infty S_p e^{-s\eta|z-z_0|} J_0(s\xi r)\,\xi\,d\xi$$

$$\pm a_r s^2\bar{F}(s) \int_0^\infty S_p' e^{-s\eta|z-z_0|} J_1(s\xi r)\xi\,d\xi$$

$$\bar{\chi}(\underset{\sim}{r},s;\underset{\sim}{a}) = -a_\theta s^2\bar{F}(s) \int_0^\infty S_H e^{-s\zeta|z-z_0|} J_1(s\xi r)\,d\xi$$

$$\bar{\psi}(r,s;a) = -a_z s\bar{F}(s) \int_o^\infty S_v e^{-s\zeta|z-z_o|} J_0(s\xi r) \, d\xi$$

$$-a_r s\bar{F}(s) \int_o^\infty S_v' e^{-s\zeta|z-z_o|} J_1(s\xi r) \, d\xi \qquad (2.17)$$

where

$$\bar{F}(s) = F_o \bar{f}(s) / 4\pi\kappa^2 s^2 \mu r_o^2 \quad , \quad S_p = -\varepsilon \quad ,, \quad S_p' = -\varepsilon / \eta$$

$$S_H = \kappa^2/\zeta \quad , \quad S_v = \xi / \zeta \quad , \quad S_v' = \varepsilon \qquad (2.18)$$

$$\zeta = (\xi^2 + \kappa^2)^{\frac{1}{2}} , \quad \eta = (\xi^2 + 1)^{\frac{1}{2}} , \quad \varepsilon = \text{sgn}(z - z_o)$$

η and ζ are the slowness in the z-direction of the P and S waves respectively and ε is the directivity constant. Note that Eq.(2.17) completely agrees with Ceranoglu [5].

2.3. DISPLACEMENTS DUE TO A SINGLE FORCE

In studying the response of a half-space due to a point source, it is more convenient to use the cylindrical coordinates (r, θ, z). Using Eq.(2.5) and (2.7), the relations between the displacements and the potentials can be written as [2]

$$u_r = \frac{\partial\phi}{\partial r} + \frac{\partial^2\psi}{\partial r\partial z} + \frac{1}{r}\frac{\partial\chi}{\partial\theta}$$

$$u_\theta = \frac{1}{r}\frac{\partial\phi}{\partial\theta} + \frac{1}{r}\frac{\partial^2\psi}{\partial\theta\partial z} - \frac{\partial\chi}{\partial r} \qquad (2.19)$$

$$u_z = \frac{\partial\phi}{\partial z} + \frac{\partial^2\psi}{\partial_z^2} - \kappa^2\frac{\partial^2\psi}{\partial t^2}$$

Note that in cylindrical coordinates

$$\nabla^2 = \frac{\partial^2}{\partial r^2} + \frac{1}{r}\frac{\partial}{\partial r} + \frac{1}{r^2}\frac{\partial^2}{\partial\theta^2} + \frac{\partial^2}{\partial z^2}$$

Substituting the potentials from Eq.(2.17) into Eq.(2.19), one can obtain the vertical displacement as

$$\bar{u}_z(\underset{\sim}{r},s;\underset{\sim}{a}) = s^3\bar{F}(s)\ \{a_z \int_o^\infty S_p D_{zp} e^{-s\eta|z-z_0|} J_0(s\xi r)\ \xi\ d\xi$$

$$+ a_z \int_o^\infty S_v D_{zv} e^{-s\zeta|z-z_0|} J_0(s\xi r)\ \xi\ d\xi$$

$$+ a_r \int_o^\infty S_p' D_{zp} e^{-s\eta|z-z_0|} J_1(s\xi r)\ \xi\ d\xi$$

$$+ a_r \int_o^\infty S_v' D_{zv} e^{-s\zeta|z-z_0|} J_1(s\xi r)\ \xi\ d\xi\}$$

(2.20)

To express the above equation in a simpler way, let one integral represent both P and SV contributions and suppress the subscripts p and v in both the source and receiver functions. Hence, Eq.(2.20) can be written as

$$\bar{u}_{zj}(\underset{\sim}{r},s;\underset{\sim}{a}) = s^3\bar{F}(s)\ \{a_z \int_o^\infty S_j D_{zj} e^{-sh_j(z,\xi)} J_0(s\xi r)\ \xi\ d\xi$$

(2.21a)

$$+ a_r \int_o^\infty S_j' D_{zj} e^{-sh_j(z,\xi)} J_1(s\xi r)\ \xi\ d\xi\}$$

$$\bar{u}_{rj}(\underset{\sim}{r},s;\underset{\sim}{a}) = s^3\bar{F}(s) \{a_z \int_0^\infty S_j^! D_{rj} e^{-sh_j(z,\xi)} \xi\, J_1(s\xi r)\, \xi\, d\xi$$

$$-a_r \int_0^\infty S_j^! D_{rj} e^{-sh_j(z,\xi)} J_0(s\xi r)\, \xi\, d\xi\}$$

(2.21b)

$$+a_r \frac{s^2}{r} \bar{F}(s) \{ \int_0^\infty S_j^! D_{rj} e^{-sh_j(z,\xi)} J_1(s\xi r)\, d\xi$$

$$+\int_0^\infty S_{Hj} D_{rHj} e^{-sh_j(z,\xi)} J_1(s\xi r)\, d\xi\}$$

$$\bar{u}_{\theta j}(\underset{\sim}{r},s;\underset{\sim}{a}) = -a_\theta \frac{s^2}{r} \bar{F}(s) \{ \int_0^\infty S_j^! D_{\theta j} e^{-sh_j(z,\xi)} J_1(s\xi r)\, d\xi$$

$$+ \int_0^\infty S_{Hj} D_{\theta Hj} e^{-sh_j(z,\xi)} J_1(s\xi r)\, d\xi \}$$

(2.21c)

$$+a_\theta s^3 \bar{F}(s) \int_0^\infty S_{\theta Hj} D_{\theta Hj} e^{-sh_j(z,\xi)} J_0(s\xi r)\, \xi\, d\xi$$

where

$$D_{zp} = -\epsilon\eta \qquad , \qquad D_{zv} = -\xi \quad .$$

$$D_{rp} = D_{\theta p} = -\xi \quad , \quad D_{rv} = D_{\theta v} = -\epsilon\zeta \quad , \quad D_{rH} = D_{\theta H} = 1$$

(2.22)

$$h_j(z,\xi) = \begin{cases} \eta|z-z_0| & \text{for P-waves} \\ \zeta|z-z_0| & \text{for S-waves} \end{cases}$$

Note that S and D denote the source and receiver functions respectively. The subscripts r, θ, z denote the directions of the displacements, and p, v, H the P, S and SH waves respectively. The transient response of the unbounded medium can now be obtained by simply taking the inverse Laplace transform of the expressions given in Eq.(2.21).

METHOD OF GENERALIZED RAYS AND
SOLUTIONS FOR A HALF SPACE

In a bounded medium, waves emitted by the source travel along different paths before they reach the receiver. Some of the rays travel the distance between the source and the receiver directly while some get reflected by the boundaries. The method of generalized rays is based on expressing the solution in terms of rays which follow different paths.

In this section a brief history of the method together with the expressions for the reflection coefficients will be given. Each ray is identified with a source and a receiver function together with different combinations of the reflection coeffients. The final solution is then obtained by summing up all possible rays. To get the inverse Laplace transform of the rays, Cagniard's method will be used. As each ray has a unique arrival time, a finite number of them are to be added up to get the transient solution.

3.1. METHOD OF GENERALIZED RAYS, A SURVEY OF LITERATURE

One of the approaches to study the response of a medium under any kind of excitation is to use the theory of normal modes. There, the complete solution of the potentials ϕ, ψ and X of Eq.(2.9) are found with two unknown coefficients for each which are determined   by applying the boundary conditions. Taking the inverse transform, the solution is found in terms of a summation with infinite number of terms. Hence, the accuracy of the results are limited with the number of terms taken in the summation.

An alternative method is known as the generalized ray theory

where the total displacement is expressed in terms of the contributions due to different rays travelling along different paths. Summing up all the possible rays, one can obtain the final solution.

The generalized ray theory was applied to the propagation of elastic waves by Cagniard [4] , when he studied the transient waves in two half-spaces welded together. Through a series of contour deformations and change of integration variables , he was able to find the inverse transform of the expressions for each ray.

Lamb [12] solved the buried force problem in a half-space when he studied the propagation of earth tremors over the surface of the earth. There, he completed the inversion of Fourier transform into the time domain by changing the integration variables in a manner very similar to Cagniard's. Later on, Pekeris and Lifson [20] solved the buried and surface source problems in a half-space. Lapwood [13] and Garvin [9] formulated the buried line source problem using the generalized ray theory and Cagniard's method. Tangential surface load over a half-space was studied by Chao [7].

On the other hand, Norwood [16] studied the case of rectangular load and proposed a method to remove the singularities that are along the integration path which made the analytical solution for the case of loads applied over finite regions, possible. Norwood [17, 18], also, studied the cases of a semi infinite line, a finite line, a quadrant and rectangular loadings acting at the surface of a half-space using the Cagniard's method.

The generalized ray theory was also applied to the plate problems by Sherwood [21], Spencer [22] and recently by Ceranoglu [5], and Pao and Gajewski [19] applied the method to a layered media.

Until 1960, the individual ray integrals in the generalized ray theory were found by using the Bromwich expansion of the exact

solution. This procedure gets tedious for a layered media problem. Spencer [22] showed that the integral solution for each of the multiply reflected and transmitted rays in a layered media can be found by a ray grouping technique. In that technique, the rays are grouped effectively disregarding their mode conversion history. Wu [24] and Norwood [16] used this technique together with Cagniard's method in solving the problem of the propagation of transient waves in an elastic thick plate under an arbitrary loading.

3.2. REDUCED BOUNDARY CONDITIONS AT A PLANE SURFACE

The boundary conditions of Eq.(2.3) for a traction free surface reduces to

$$\underset{\sim}{\sigma} \cdot \underset{\sim}{n} = 0 \tag{3.1}$$

In cylindrical coordinates, the components of the stress tensor are related to the displacement potentials through the expressions [2,5]

$$\sigma_{zz} = \frac{\kappa^2 - 2}{\kappa^2} \frac{\partial^2 \phi}{\partial t^2} + \frac{2}{\kappa^2} \cdot \frac{\partial}{\partial z} \left[\frac{\partial \phi}{\partial z} + \frac{\partial^2 \psi}{\partial z^2} - \kappa^2 \frac{\partial^2 \psi}{\partial t^2} \right]$$

$$\sigma_{rz} = \frac{1}{\kappa^2} \frac{\partial}{\partial r} \left[2 \frac{\partial \phi}{\partial z} + 2 \frac{\partial^2 \psi}{\partial z^2} - \kappa^2 \frac{\partial^2 \psi}{\partial t^2} \right] + \frac{1}{\kappa^2 r} \frac{\partial}{\partial \theta} \frac{\partial \chi}{\partial z} \tag{3.2}$$

$$\sigma_{\theta z} = \frac{1}{\kappa^2 r} \frac{\partial}{\partial \theta} \left[2 \frac{\partial \phi}{\partial z} + 2 \frac{\partial^2 \psi}{\partial z^2} - \kappa^2 \frac{\partial^2 \psi}{\partial t^2} \right] - \frac{1}{\kappa^2} \frac{\partial}{\partial r} \frac{\partial \chi}{\partial z}$$

If the equation of the surface is $z=\ell$, where ℓ is a constant, then Eq. (3.1) becomes

$$\sigma_{zz} = 0 \quad \text{at } z = \ell \tag{3.3a}$$

$$\sigma_{rz} = 0 \quad \text{at } z = \ell \tag{3.3b}$$

$$\sigma_{\theta z} = 0 \quad \text{at } z = \ell \tag{3.3c}$$

Substituting Eq.(3.2) into Eq.(3.3), one obtains the expressions for the boundary conditions. To express the last two boundary condition in reduced form, consider a function $\sigma(r,\theta)$ such that

$$(2\frac{\partial\phi}{\partial z} + 2\frac{\partial^2\psi}{\partial z^2} - \kappa^2\psi) \Big|_{z=\ell} = \frac{\partial\sigma}{\partial\theta}$$

$$\tag{3.4}$$

$$(\frac{\partial\chi}{\partial z})\Big|_{z=\ell} = -r\frac{\partial\sigma}{\partial r}$$

Then the boundary condition (3.3b) is satisfied identically, and the condition (3.3c) will be satisfied if the function $\sigma(r,\theta)$ satisfies the equation

$$\frac{\partial^2\sigma}{\partial r^2} + \frac{1}{r}\frac{\partial\sigma}{\partial r} + \frac{1}{r^2}\frac{\partial^2\sigma}{\partial\theta^2} = 0 \tag{3.5}$$

which is the Laplacian of $\sigma(r,\theta)$ in the plane $z=\ell$. Hence, $\sigma(r,\theta)$ is a harmonic function. Since the solution has to be bounded at infinity, Liouville's theorem [15] states that $\sigma(r,\theta)$ is constant. Therefore, the boundary conditions of Eq.(3.3) reduces to

$$\{(\kappa^2-2)\ddot{\phi} + 2\frac{\partial}{\partial z}(\frac{\partial\phi}{\partial z} + \frac{\partial^2\psi}{\partial z^2} - \kappa^2\ddot{\psi})\}\Big|_{z=\ell} = 0$$

$$\Sigma\Big|_{z=\ell} \equiv (2\frac{\partial\phi}{\partial z} + 2\frac{\partial^2\psi}{\partial z^2} - \kappa^2\ddot{\psi})\Big|_{z=\ell} = 0 \tag{3.6}$$

$$\Sigma_H\Big|_{z=\ell} \equiv (\frac{\partial\chi}{\partial z})\Big|_{z=\ell} = 0$$

where Σ shows the component of the stresses σ_{rz} and $\sigma_{\theta z}$ due to P-wave and S-wave, and Σ_H due to SH-wave. Note that Ceranoglu [5] and Chandra [6] used the same boundary conditions. Using these boundary conditions, the reflection coefficients for the traction free plane surface of the half-space can be found.

3.3 REFLECTION COEFFICIENTS AT A FREE SURFACE

Waves emitted by a buried source in a half-space act like those in an infinite medium until they reach to a point on the surface where they are reflected and transmitted. Therefore, the particular solutions found in Chapter II are valid for the incident waves on the surface. Using Eq.(3.2) incident stresses can also be found.

The reflection coefficients at a free surface will be derived considering the case of a concentrated single force inside a half space. Substitution of Eq. (2.17) into Eq.(3.2) after taking Laplace transform yields

$$
\sigma_{zz}^{(inc)} = s^4 F(s) \{ a_z \int_0^\infty S_p D_{zz}^{(p)} e^{-s\eta|z-z_0|} J_0 \, \xi \, d\xi
$$

$$
+ a_z \int_0^\infty S_v D_{zz}^{(v)} e^{-s\zeta|z-z_0|} J_0 \, \xi \, d\xi
$$

$$
+ a_r \int_0^\infty S_p' D_{zz}^{(p)} e^{-s\eta|z-z_0|} J_1 \, \xi \, d\xi
$$

$$
+ a_r \int_0^\infty S_v' D_{zz}^{(v)} e^{-s\zeta|z-z_0|} J_1 \, \xi \, d\xi \}
$$

(3.7)

where

$$
D_{zz}^{(p)} = (\xi^2 + \zeta^2)/\kappa^2 \quad , \quad D_{zz}^{(v)} = 2\varepsilon\zeta\xi/\kappa^2 \tag{3.8}
$$

Similar expressions can be obtained for $\bar{\Sigma}^{(inc)}$ and $\bar{\Sigma}^{(inc)}$ using Eq.(3.6).

In a half-space, $z \geq 0$, the waves that are generated at $z = z_0$ will be reflected when they reach the surface $z=0$. On a plane surface, a P or S wave will be reflected both as a P and S wave, which is known as mode conversion. However, a SH-wave will be reflected as a SH-wave only. The corresponding quantities for the reflected waves can be expressed as

$$
\sigma_{zz}^{(ref)} = s^4 F(s) \{ [a_z \int_0^\infty S_p R^{pp} D_{zz}^{(p)} e^{-s\eta(z+z_0)} J_0 \, \xi \, d\xi
$$

$$
+ a_z \int_0^\infty S_p' R^{pp} D_{zz}^{(p)} e^{-s\eta(z+z_0)} J_1 \, \xi \, d\xi]
$$

$$
+ [a_z \int_0^\infty S_p R^{ps} D_{zz}^{(v)} e^{-s(\eta z_0 + \zeta z)} J_0 \, \xi \, d\xi
$$

$$
+ \bar{a}_r \int_0^\infty S_p' R^{ps} D_{zz}^{(v)} e^{-s(\eta z_0 + \zeta z)} J_1 \, \xi \, d\xi]
$$

$$
+ [a_z \int_0^\infty S_v R^{ss} D_{zz}^{(v)} e^{-s\zeta(z+z_0)} J_0 \, \xi \, d\xi
$$

$$
+ a_r \int_0^\infty S_v' R^{ss} D_{zz}^{(v)} e^{-s\zeta(z+z_0)} J_1 \, \xi \, d\xi]
$$

$$
+ [a_z \int_0^\infty S_v R^{sp} D_{zz}^{(p)} e^{-s(\zeta z_0 + \eta z)} J_0 \, \xi \, d\xi
$$

$$
+ a_r \int_0^\infty S_v' R^{sp} D_{zz}^{(p)} e^{-s(\zeta z_0 + \eta z)} J_1 \, \xi \, d\xi] \}
$$

(3.9)

Note that each bracket in the above expression represents a different ray; the first is the incident P reflected P, the second is the incident P reflected S, the third is the incident S reflected S, and the fourth is the incident S reflected P wave. These different rays are identified

with their reflection coefficients R^{pp}, $R^{\overline{ps}}$, R^{ss}, R^{sp} respectively. Similar expressions can be written for $\bar{\Sigma}^{(ref)}$ and $\bar{\Sigma}_H^{(ref)}$.

The boundary conditions has to be satisfied by the total wave field which is the sum of incident and reflected waves. Adding the two and setting z=0 yields

$$\bar{\sigma}_{zz}|_{z=0} = \bar{\sigma}_{zz}^{(inc)}|_{z=0} + \bar{\sigma}^{(ref)}|_{z=0} = 0$$

$$\bar{\Sigma}|_{z=0} = \bar{\Sigma}^{(inc)}|_{z=0} + \bar{\Sigma}^{(ref)}|_{z=0} = 0 \qquad (3.10)$$

$$\bar{\Sigma}_H|_{z=0} = \bar{\Sigma}_H^{(inc)}|_{z=0} + \bar{\Sigma}_H^{(ref)}|_{z=0} = 0$$

one can obtain the generalized reflection coefficients for a traction free plane surface as [5]

$$R^{pp} = R^{ss} = [4\eta\zeta\xi^2 + (\xi^2+\zeta^2)^2]/\Delta r$$

$$R^{ps} = -4\eta\xi(\xi^2+\zeta^2)/\Delta r$$

$$R^{sp} = (\frac{\zeta}{\eta})R^{ps} \qquad (3.11)$$

$$R^H = 1$$

$$\Delta r = 4\eta\zeta\xi^2 - (\xi^2+\zeta^2)^2$$

3.4. RAY SOLUTIONS FOR A HALF SPACE

The complete solution of the displacements due to transient waves in a half-space is obtained by combining the particular solutions of sec.(2.3) and the reflection rays of sec.(3.3).

Consider a concentrated force acting at a point $(0,0,z_0)$ with the receiver at a point Q (r,θ,z), (Fig.2). It is clear that the waves reach to the receiver through different paths. First one is the path 1 where a direct P-wave and a direct S-wave travel along. Note that the P-wave reaches to the receiver before the S-wave. As there is no reflection in path 1, these waves are the direct waves just like in an unbounded medium, (Fig.2). The waves that are reflected at the surface will reach to the receiver travelling along the paths similar to path 2. The total vertical displacement on the surface of the half-space due to the waves travelling along path 2 is

$$\bar{u}_z^{(ref)}(r,s;a) = s^3 F(s) \left\{ [a_z \int_0^\infty S_p R^{pp} D_{zp} e^{-s\eta(z+z_0)} J_0 \, \xi \, d\xi \right.$$

$$+ a_r \int_0^\infty S_p' R^{pp} D_{zp} e^{-s\eta(z+z_0)} J_1 \, \xi \, d\xi]$$

$$+ [a_z \int_0^\infty S_p R^{ps} D_{zv} e^{-s(\eta z_0 + \zeta z)} J_0 \, \xi \, d\xi$$

$$+ a_r \int_0^\infty S_p' R^{ps} D_{zv} e^{-s(\eta z_0 + \zeta z)} J_1 \, \xi \, d\xi]$$

$$+ [a_z \int_0^\infty S_v R^{ss} D_{zv} e^{-s\zeta(z+z_0)} J_0 \, \xi \, d\xi$$

$$+ a_r \int_0^\infty S_v' R^{ss} D_{zv} e^{-s\zeta(z+z_0)} J_1 \, \xi \, d\xi]$$
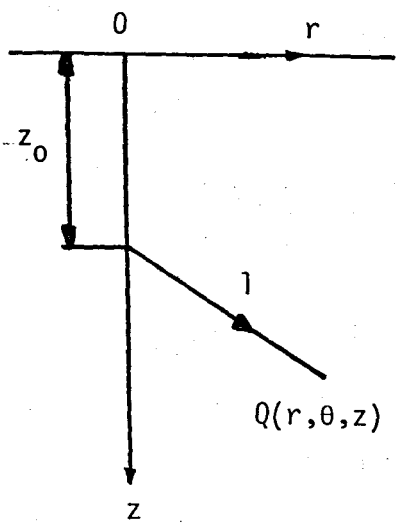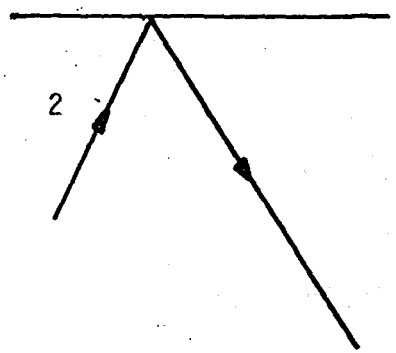
(a) Direct wave, Path 1   (b) Reflected wave, Path 2

$r_0/z_0 < 1/\sqrt{2}$ $r_0/z_0 = 1/\sqrt{2}$ $r_0/z_0 > 1/\sqrt{2}$
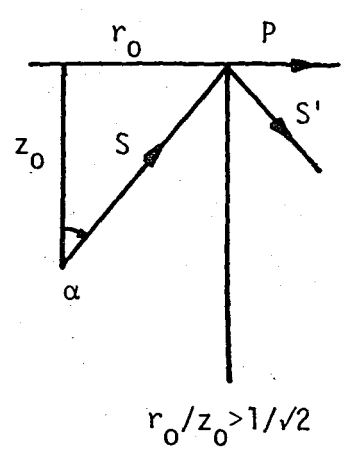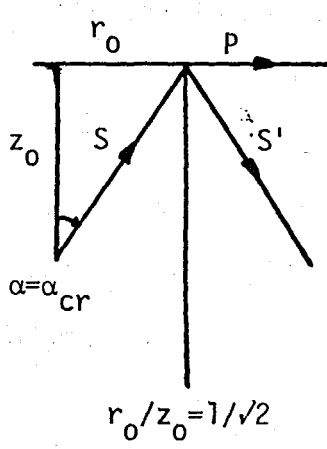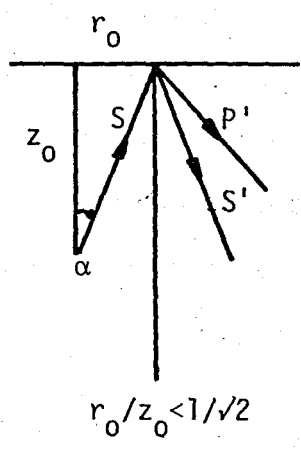
$$\tan\alpha = r_0/z_0 \ , \ \tan\alpha_{cr} = 1/\sqrt{2}$$

(c) Head wave

Figure 2. Rays in a half-space

$$+[a_z \int_0^\infty S_v R^{sp} D_{zp} e^{-s(\zeta z_0 + \eta z)} J_0 \, \xi \, d\xi$$

$$+ a_r \int_0^\infty S_v' R^{sp} D_{zp} e^{-s(\zeta z_0 + \eta z)} J_1 \, \xi \, d\xi]\} \qquad (3.12)$$

As stated earlier, each bracket in this expression represents a single ray propagating along path 2. The phase of each ray is given by the argument of the exponential term. In general the phase function is written in the form

$$-sh = -s(\eta z_p + \zeta z_s) \qquad (3.13)$$

where z_p and z_s are the total vertical components of the segments in a particular ray, travelling in P and S modes respectively. As each ray has a unique arrival time, only the ones that arrive prior to the time of interest are considered.

The key point in Eq.(3.12) is that the terms in brackets are all similar in nature, hence, one can write the contribution of the jth ray to the vertical displacement as

$$\bar{u}_{zj}(\underline{r}, s; \underline{a}) = s^3 \bar{F}(s) \, \{a_z \int_0^\infty S_j \Pi_j D_{zj} e^{-sh_j} J_0 \xi \, d\xi$$

$$\qquad (3.14a)$$

$$+ a_r \int_0^\infty S_j' \Pi_j D_{zj} e^{-sh_j} J_1 \xi \, d\xi \}$$

Similarly $\bar{u}_{rj}$ and $\bar{u}_{\theta j}$ can be written as

$$\bar{u}_{rj}(\underset{\sim}{r},s;\underset{\sim}{a}) = s^3\bar{F}(s) \{a_z \int_0^\infty S_j \Pi_j D_{rj} e^{-sh_j} J_1 \xi d\xi$$

$$-a_r \int_0^\infty S'_j \Pi_j D_{rj} e^{-sh_j} J_0 \xi d\xi\}$$

$$+\frac{s^2}{r}\bar{F}(s) \, a_r \, \{\int_0^\infty S'_j \Pi_j D_{rj} e^{-sh_j} J_1 d\xi$$

$$+\int_0^\infty S_{Hj} \Pi_{Hj} D_{rHj} e^{-sh_{Hj}} J_1 d\xi\} \tag{3.14b}$$

$$\bar{u}_{\theta j}(\underset{\sim}{r},s;\underset{\sim}{a}) = -a_\theta \frac{s^2}{r}\bar{F}(s) \int_0^\infty S'_j \Pi_j D_{\theta j} e^{-sh_j} J_1 d\xi$$

$$+\{a_\theta s^3\bar{F}(s) \int_0^\infty S_{Hj} \Pi_{Hj} D_{\theta Hj} e^{-sh_{Hj}} J_0 \xi d\xi$$

$$-a_\theta \frac{s^2}{r}\bar{F}(s) \int_0^\infty S_{Hj} \Pi_{Hj} D_{\theta Hj} e^{-sh_{Hj}} J_1 d\xi\} \tag{3.14c}$$

where Π's are the reflection coefficient for the jth ray in a half-space.

Therefore, it is understood that each ray is expressed by a definite source, receiver and phase function, and a reflection coefficient. Along path 1, $\Pi_j = \Pi_{Hj} = 1$ as there is no reflection. Along path 2, $\Pi_j = R^{pp}$, R^{ps}, R^{ss} and R^{sp} for the mentioned reflected rays in P and S modes and $\Pi_{Hj} = 1$ for the reflected SH-waves.

3.5. EXPRESSIONS FOR THE SURFACE SOURCE AND RECEIVER FUNCTIONS

Until now, we discussed the case in which both the source and the receiver were buried in a half-space. Now, the three other cases, in which either the source or the receiver or both of them

simultaneously on the surface, will be discussed.

3.5.1.Surface Source

To get the surface source function, we consider the buried source and buried receiver case. Both P and S rays are emitted by the source, and after reflection in addition to the direct P and S waves, PP, PS, SS and SP waves will also reach to the receiver. Consider only the ray integrals for the P, PP and SP waves. In the limit as z_0 approaches zero, these three integrals will combine and result in a single integral with a new source function, (Fig.3)

$$S_p^* = S_p + S_p R^{pp} + S_v R^{sp} \qquad (3.15)$$

This is the ray travelling the distance between the source and the receiver as a P-wave. Considering the ray integrals for S, SS and PS waves and going through a similar procedure, an expression for the source function of the ray travelling as a S-wave between the source and the receiver can be obtained.

$$S_v^* = S_v + S_v R^{ss} + S_p R^{ps} \qquad (3.16)$$

Recalling that no mode conversion takes place for the SH-wave, the surface source function, S_H^*, for such waves is obtained from the SH-component of the integrals for S and SS waves. Hence

$$S_H^* = S_H + S_H R^H = 2S_H \qquad (3.17)$$

3.5.2.Surface Receiver

The expressions for the surface receiver functions can be obtained by going through a similar procedure outlined in the previous section. For example, considering the integrals for the
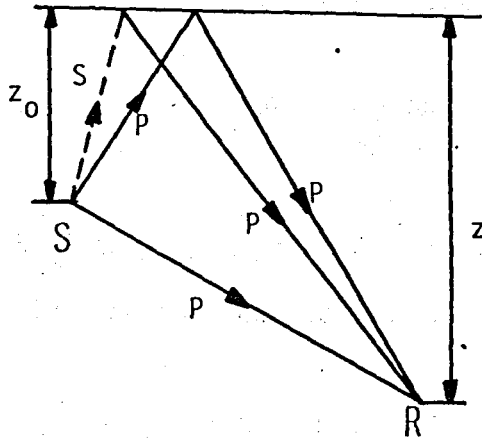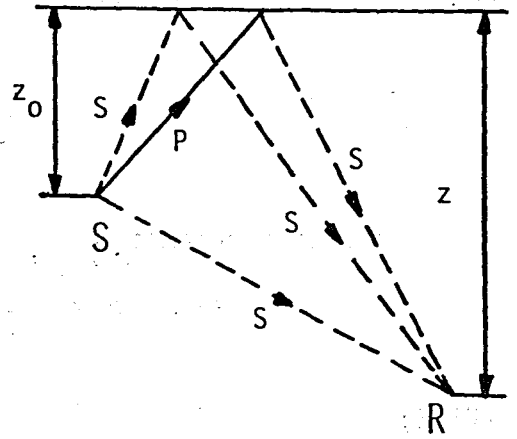
(a) P-source   (b) S-source

Figure 3. Rays used in the derivation of surface source functions.
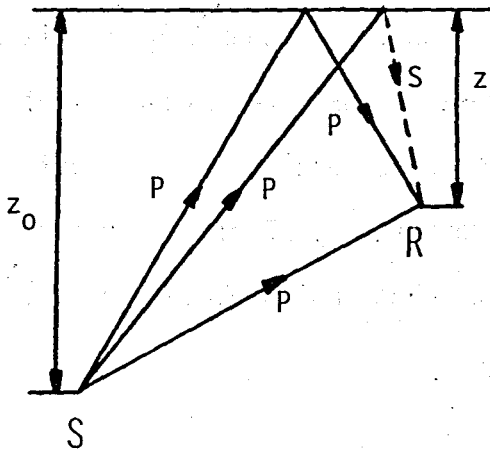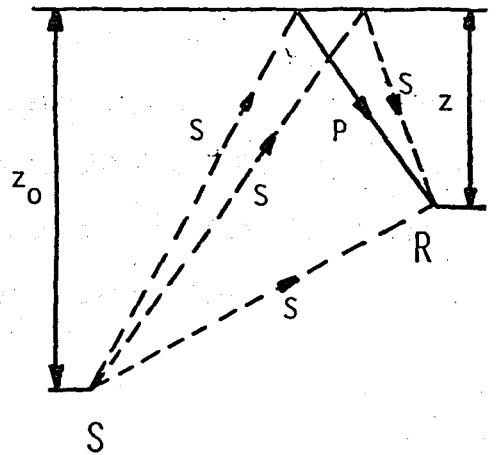
(a) P-receiver   (b) S-receiver

Figure 4. Rays used in the derivation of surface receiver functions.

P, PP and PS rays and taking the limit as z approaches to zero, yields a single integral with a P-wave receiver function of the form, (Fig.4)

$$D_{\alpha p}^{*} = D_{\alpha p} + D_{\alpha p}R^{pp} + D_{\alpha v}R^{ps} \qquad (3.18)$$

Similarly, integrals for the rays S, SS and SP combine together to give the surface receiver function for the SV-wave as

$$D_{\alpha v}^{*} = D_{\alpha v} + D_{\alpha v}R^{ss} + D_{\alpha p}R^{sp} \quad . \qquad (3.19)$$

Accordingly, for SH-waves we have

$$D_{\alpha H}^{*} = D_{\alpha H} + D_{\alpha H}R^{H} = 2D_{\alpha H} \qquad (3.20)$$

3.5.3. The Source and the Receiver on the Surface

The expressions for the case, in which both the source and the receiver are on the surface, can be obtained by going through a similar procedure outlined for the surface source case. This time, in the limit, as z and z_0 approaches to zero, a P and a S wave travelling from the source to the receiver can be obtained. One can get the same result in Eq.(3.14), replacing the source function with a surface source function, and taking an inside receiver function and $\Pi = 1$.

CAGNIARD'S METHOD AND

THE INVERSION OF LAPLACE TRANSFORM

The general expressions for the displacements due to a concentrated force was given by Eq.(3.14). All of the integrals appearing in these expressions are of the two kind

$$\bar{I}_0(r,z,s) = \int_0^\infty E_1(\xi) \; \xi \; J_0(s\xi r)e^{-s(z_p\eta+z_s\zeta)} \; d\xi$$

$$(4.1)$$

$$\bar{I}_1(r,z,s) = \int_0^\infty E_2(\xi) \; \xi^2 J_1(s\xi r)e^{-s(z_p\eta+z_s\zeta)} \; d\xi$$

where E_1^- and E_2 are the even functions of ξ involving the source and the receiver functions, and the reflection coefficient. The coefficients of these integrals are of the form $s^n F(s)$, therefore, after finding the inverse transform of I_0 and I_1, one can obtain the final solution through a convolution integral.

4.1. INTEGRAL REPRESENTATION IN THE t-PLANE

The representation of the integrals in the ξ-plane are given by Eq.(4.1). There, the key point in the application of Cagniard's method is to use the integral representation of Bessel functions, J_0 and J_1. These are, (Abromovitz and Stegun[1]),

$$J_0(z) = \frac{2}{\pi} \; \text{Re} \int_0^{\pi/2} e^{izcos\omega}d\omega$$

$$(4.2)$$

$$J_1(z) = \frac{2}{\pi} \; \text{Im} \int_0^{\pi/2} e^{izcos\omega}cos\omega \, d\omega$$

Using the above expressions in Eq.(4.1) and changing the order of integration, as the integrals in ξ are uniformly convergent for all values of ω between o and $\pi/2$, we get

$$\bar{I}_0(r,z,s) = \frac{2}{\pi} \, \text{Re} \int_0^{\pi/2} d\omega \int_0^\infty E_1(\xi) \, e^{-s(-i\xi r\cos\omega + z_p\eta + z_s\zeta)} \, \xi \, d\xi$$

(4.3)

$$\bar{I}_1(r,z,s) = \frac{2}{\pi} \, \text{Im} \int_0^{\pi/2} \cos\omega \, d\omega \int_0^\infty \xi E_2(\xi) \, e^{-s(-i\xi r\cos\omega + z_p\eta + z_s\zeta)} \, \xi \, d\xi$$

The most important point of the Cagniard's method is to make the following transformation

$$t = -i\xi r\cos\omega + z_p\eta + z_s\zeta \equiv g(r,z;\xi)$$

(4.4)

In the complex ξ-plane, $g(r,z;\xi)$ is a multivalued function with branch points at $\xi=\pm i$ due to the second term and $\xi=\pm i\kappa$ due to the third term in Eq.(4.4). Introducing the branch cuts as shown in Fig.(5a), it becomes single valued. These branches are chosen such that if ξ is real and positive, the radicals are positive.

Considering ξ as a complex variable, one can make the transformation of complex ξ-plane to complex t-plane, (Fig.5b). The original line of integration, the real ξ-axis, is mapped into the curve A'B' in the t-plane. The origin, A', of this curve corresponds to the value of $t=t_A$ where

$$t_A = z_p + z_s\kappa$$

Note that the curve A'B' has an asymptote of the form

$$t = \frac{-x}{z_p + z_s}$$

(4.5)

where $x=r\cos\omega$. On the other hand, by substituting $\xi=i\ell$, one can make
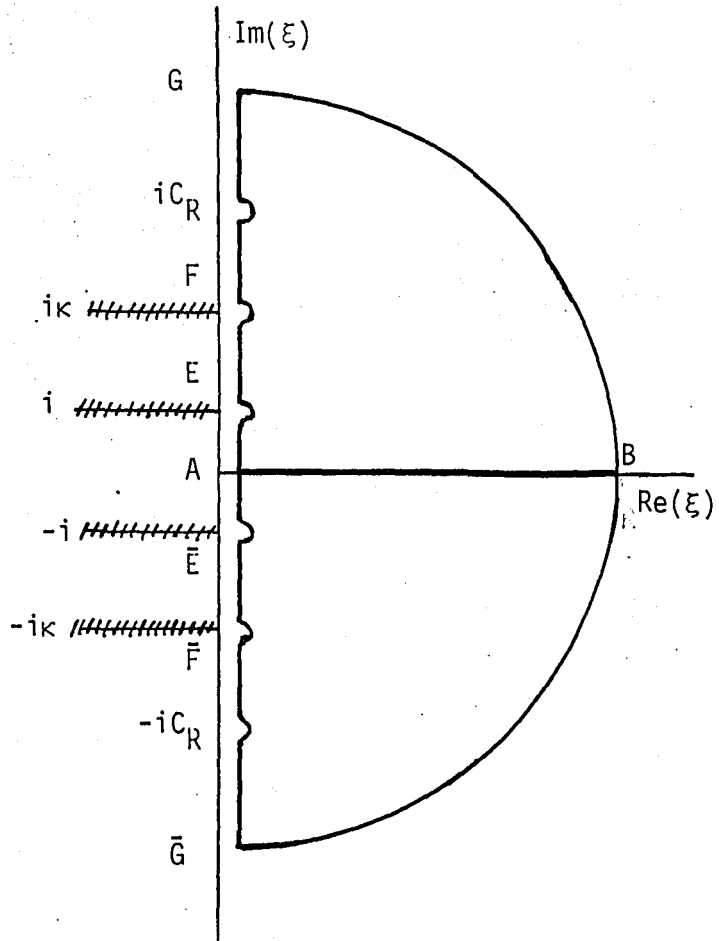
Figure 5a. ξ-plane
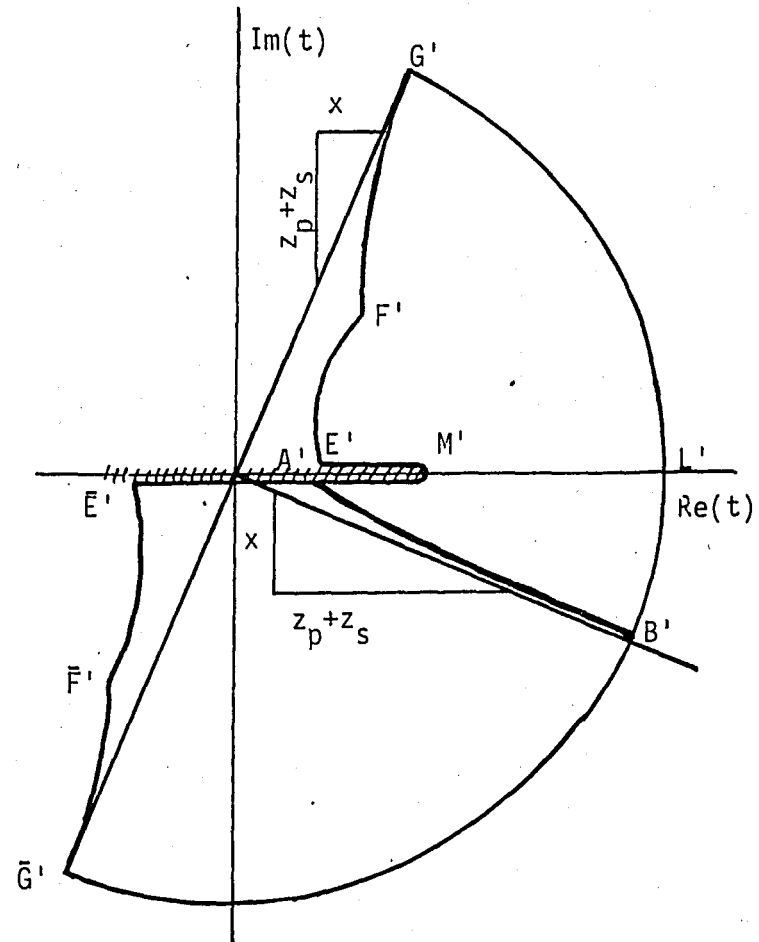
Figure 5b. Map of the ξ-plane in the t-plane.

the transformation of the imaginary ξ-axis,

$$t = x\ell + z_p(1-\ell^2)^{\frac{1}{2}} + z_s(\kappa^2-\ell^2)^{\frac{1}{2}} \tag{4.6}$$

Equation (4.6) shows that the points on the imaginary ξ-axis with $|\ell|<1$ if $z_p\neq0$ and the points with $|\ell|<\kappa$ if $z_p=0$ will lie on the real t-axis. It can be shown that as $\ell\to\pm\infty$, t approaches an asymptote given by

$$t = \frac{z_p + z_s}{x} \tag{4.7}$$

From the behavior of Eq.(4.6), the points that are mapped into the real t-axis may be double valued if there is a stationary point M. This point is an extremum for $g(r,z;\xi)$ satisfying the relation

$$\left(\frac{\partial t}{\partial \xi}\right)_\omega = -ix + \frac{z_p\xi}{\eta} + \frac{z_s\xi}{\zeta} = 0 \tag{4.8}$$

This equation has the root $\xi= i\ell_M$. Considering the surface response of a half-space, we either have z_p or z_s equal to zero, hence, this equation can be solved for ℓ_M

$$\ell_M = \frac{r\alpha}{(z_0^2 + r^2)^{\frac{1}{2}}} \tag{4.9}$$

where $z_0=z_p$ and $\alpha=1$ for the P-waves, and $z_0=z_s$ and $\alpha=\kappa$ for the S-waves To render the single valuedness of the mapping, a branch cut is introduced along the real t-axis starting at the point t_M. Thus, the segment AME of the positive imaginary ξ-axis is mapped into A'M'E' in the t-plane where A'M' lies below the branch line and M'E' above.

(Fig.5b). The point t_M is given by

$$t_M = x\ell_M + z_0(\alpha^2 - \ell_M^2)^{\frac{1}{2}} \tag{4.10}$$

Therefore, using the transformation given by Eq.(4.4), the expressions for I_0 and I_1 become

$$\bar{I}_0(r,z,s) = \frac{2}{\pi} \text{Re} \int_0^{\pi/2} d\omega \int_{A'B'} E_1[\xi(t)] \, \xi(t) \, (\frac{d\xi}{dt})_\omega \, e^{-st} \, dt \tag{4.11}$$

$$\bar{I}_1(r,z,s) = \frac{2}{\pi} \text{Im} \int_0^{\pi/2} \cos\omega \, d\omega \int_{A'B'} E_2[\xi(t)]\xi^2(t) \, (\frac{d\xi}{dt})_\omega \, e^{-st} \, dt$$

4.2. INVERSION OF LAPLACE TRANSFORM AND TRANSFORMATION INTO THE ξ-PLANE

The integral representations in the complex t-plane were found in Eq.(4.11), where the new path of integration is along A'B'. Now consider the contour A'B'L'M'A'. Since there are no singularities inside this contour, the integral along this closed contour, from Cauchy's principle, is zero. Also, as B'L' is moved to infinity, the integrand of Eq.(4.11) vanishes along this portion of the contour. Therefore, A'M'L' can be taken as the new path of integration along the real t-axis, instead of A'B'. Rewriting Eq.(4.11), we have

$$\bar{I}_0(r,z,s) = \frac{2}{\pi} \text{Re} \int_0^{\pi/2} d\omega \int_{t_A}^{\infty} E_1[\xi(t)]\xi(t) \, (\frac{d\xi}{dt})_\omega \, e^{-st} \, dt \tag{4.12}$$

$$\bar{I}_1(r,z,s) = \frac{2}{\pi} \text{Im} \int_0^{\pi/2} \cos\omega \, d\omega \int_{t_A}^{\infty} E_2[\xi(t)]\xi^2(t) \, (\frac{d\xi}{dt})_\omega e^{-st} \, dt$$

The above analysis is true when $\omega \neq \pi/2$. If $\omega = \pi/2$, Eq.(4.4) becomes

$$t = z_p \eta + z_s \zeta \qquad (4.13)$$

which means that the real ξ-axis is mapped directly into the real t-axis. For this case, $t_A = t_M$; so it is understood that Eq.(4.12) is also valid for $\omega = \pi/2$. Note that, the integrals in Eq.(4.12) converge uniformly for all $0 \le \omega \le \pi/2$ and t except at $t = t_M$ where $(d\xi/dt)_\omega$ has a half order singularity. Therefore, changing the order of integration, we get

$$\bar{I}_0(r,z,s) = \int_{t_A}^{\infty} \{ \frac{2}{\pi} \, \text{Re} \int_0^{\pi/2} E_1[\xi(t;\omega)] \, \xi(t;\omega) (\frac{d\xi}{dt})_\omega d\omega \} e^{-st} \, dt$$

$$(4.14)$$

$$\bar{I}_1(r,z,s) = \int_{t_A}^{\infty} \{ \frac{2}{\pi} \, \text{Im} \int_0^{\pi/2} E_2[\xi(t;\omega)] \, \xi^2(t;\omega) (\frac{d\xi}{dt}) \cos\omega \, d\omega \} e^{-st} \, dt$$

Note that if the lower limits of integration were zero rather than t_A, the above expression would have been in the form of the Laplace transform of the quantities inside the curly bracket { }. This can be achieved by introducing a Heaviside's step function $H(t-t_A)$. Thus the inverse Laplace transform of the expressions are simply their corresponding integrands with the Heaviside's function attached to them, i.e.

$$I_0(r,z,t) = H(t-t_A) \frac{2}{\pi} \, \text{Re} \int_0^{\pi/2} E_1[\xi(t;\omega)] \, \xi(t;\omega) \, (\frac{d\xi}{dt})_\omega \, d\omega$$

$$(4.15)$$

$$I_1(r,z,t) = H(t-t_A) \frac{2}{\pi} \, \text{Im} \int_0^{\pi/2} E_2[\xi(t;\omega)] \, \xi^2(t;\omega) \, (\frac{d\xi}{dt})_\omega \cos\omega \, d\omega$$

In calculating the above integrals numerically, for each value of t, the values of ξ have to be found for different values of ω, $0 \leq \omega \leq \pi/2$. Also $(d\xi/dt)_\omega$ will have a singularity at some value of ω for each value of t. Therefore, to overcome these difficulties another change of variable is appropriate, namely the change of variable ω back to ξ. For this purpose we use the transformation given by Eq.(4.4) once more. This transformation will allow to transform the finite integral in the ω-plane into another finite integral in the ξ-plane. From Eq.(4.4)

$$\cos\omega = \frac{z_p\eta + z_s\zeta - t}{i\xi r} \qquad , \qquad r \neq 0 \qquad (4.16)$$

Note that if $\xi=0$, then $t=t_A= z_p+z_s\kappa$ (from Eq.4.4) and the above expression becomes indeterminate. Using the l'Hopitals rule, we find that $\omega \to \pi/2$ as $\xi \to 0$. For $\omega = 0$, Eq.(4.4) yields $\xi = \xi_1(r,z,t)$, where

$$t = -i\xi_1 r + z_p\eta_1 + z_z\zeta_1 \quad , \quad \eta_1 = (\xi_1^2+1)^{\frac{1}{2}} , \quad \zeta_1 = (\xi_1^2+\kappa^2)^{\frac{1}{2}} \qquad (4.17)$$

Therefore,Eq.(4.15) becomes

$$I_0(r,z,t) = H(t-t_A) \frac{2}{\pi} \text{Re} \int_{\xi_1(r,z,t)}^{0} E_1(\xi)(\frac{\partial\xi}{\partial t})_\omega (\frac{\partial\omega}{\partial\xi})_t \xi \, d\xi$$

$$(4.18)$$

$$I_1(r,z,t) = H(t-t_A) \frac{2}{\pi} \text{Im} \int_{\xi_1(r,z,t)}^{0} \xi E_2(\xi) \frac{z_p\eta+z_s\zeta-t}{i\xi r} (\frac{\partial\xi}{\partial t})_\omega (\frac{\partial\omega}{\partial\xi})_t \xi \, d\xi$$

It is understood that ξ_1 is a complex number on the contour, AML, which is the mapping of the real t-axis in the ξ-plane. The integrals of the above equation are along $AM\xi_1$ which is the finite portion of

AML, (Fig.6a and 6b).

From Eq.(4.4)

$$\left(\frac{\partial \omega}{\partial \xi}\right)_t = \frac{-ir\cos\omega + z_p \xi/\eta + z_s \xi/\zeta}{-ir\xi\sin\omega} \qquad (4.19)$$

and using Eq.(4.8) we get

$$\left(\frac{\partial \xi}{\partial t}\right)_\omega \left(\frac{\partial \omega}{\partial \xi}\right)_t = \frac{1}{-ir\xi\sin\omega} \qquad (4.20)$$

Solving Eq.(4.16) for $\sin\omega$ and substituting it in Eq.(4.20), one obtains

$$\left(\frac{\partial \xi}{\partial t}\right)_\omega \left(\frac{\partial \omega}{\partial \xi}\right)_t = \frac{-1}{iK(r,z,t;\xi)} \qquad (4.21)$$

where $K(r,z,t;\xi) = [\xi^2 r^2 + (z_p \eta + z_s \zeta - t)^2]^{\frac{1}{2}}$ $\qquad (4.22)$

Substituting Eq.(4.21) in Eq.(4.18), one obtains the expressions to be used in numerical calculations.

$$I_0(r,z,t) = H(t-t_A) \frac{2}{\pi} \text{Im} \int_0^{\xi_1} E_1(\xi) \frac{\xi}{K} d\xi$$

$$(4.23)$$

$$I_1(r,z,t) = -H(t-t_A) \frac{2}{\pi r} \text{Im} \int_0^{\xi_1} \xi E_2(\xi) \frac{z_p \eta + z_s \zeta - t}{K} d\xi$$

The K has a branch point at $\xi=\xi_1$, hence, a branch cut has to be introduced at ξ_1. The branch cut is chosen such that the real part of K is positive when real part of ξ is positive.
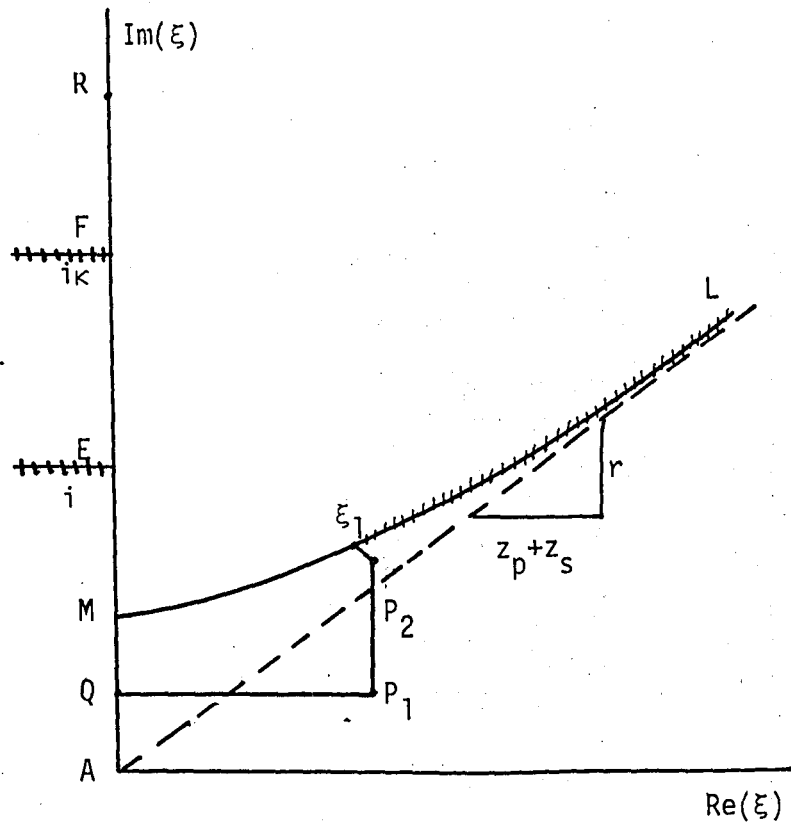
Figure 6a. Integration path for the direct
and reflected rays.
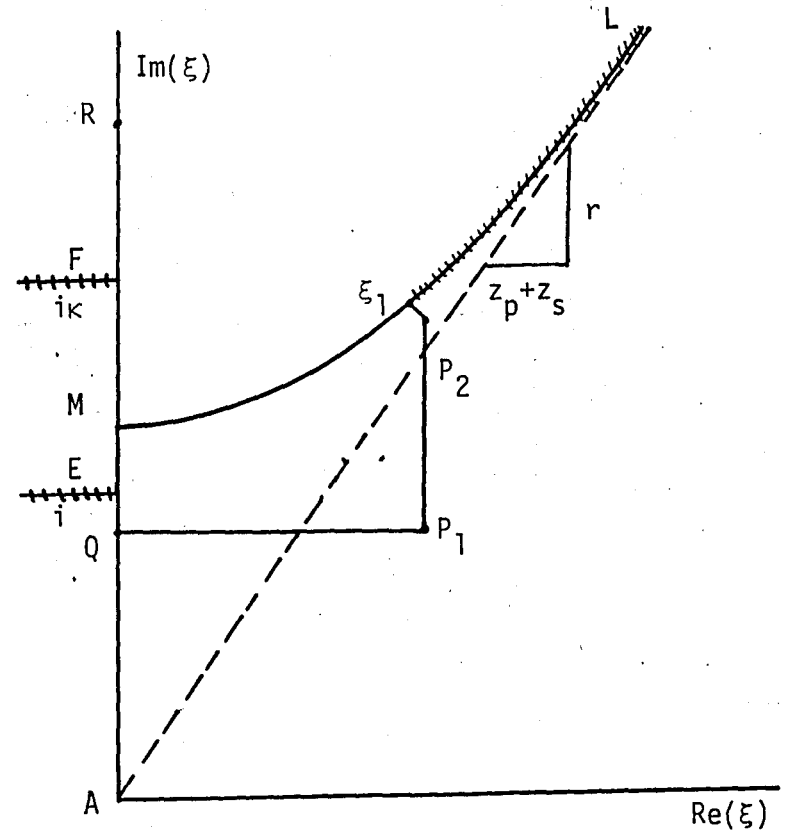
Figure 6b. Integration path for the refracted
rays when real part of ξ is not
zero.
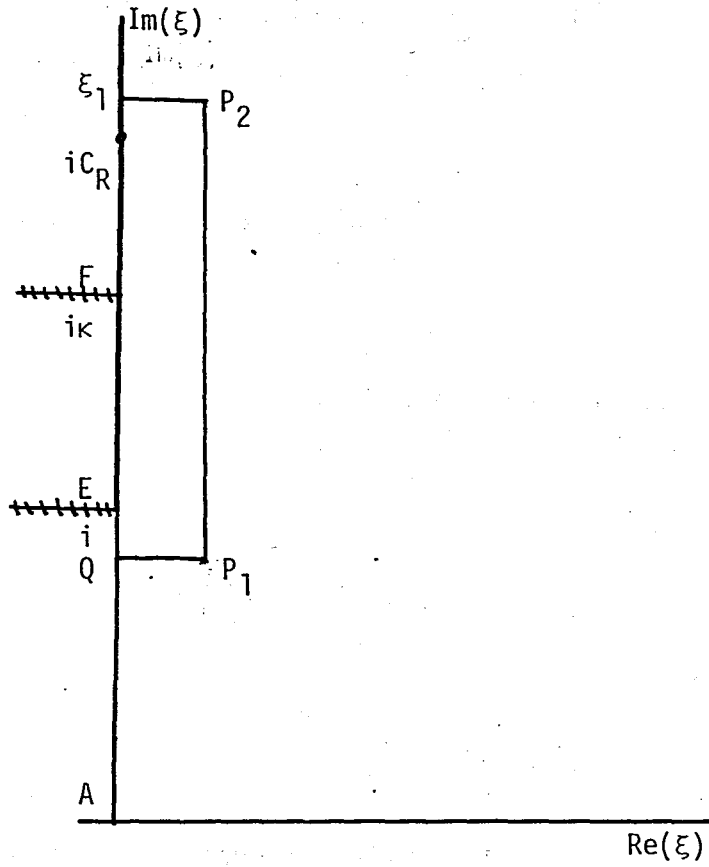
Figure 6c. Integration path for the cases of
surface source, and refracted
rays when real part of ξ is zero.

4.3. ARRIVAL TIMES OF INDIVIDUAL RAYS

The expression for the arrival time of a ray, in the case of a buried source and receiver in a half-space, can be obtained considering Eq.(4.10) as

$$t_M = \ell_M r \cos\omega + z_p(1-\ell_M^2)^{\frac{1}{2}} + z_s(\kappa^2-\ell_M^2)^{\frac{1}{2}} \tag{4.24}$$

The physical meaning of t_M is made clear by the following analysis of geometry. Let

$$\ell_M = \sin\alpha = \kappa\sin\beta \quad , \quad \alpha,\beta>0 \quad ; \quad \beta\leq\pi/2 \tag{4.25}$$

and

$$z_p\tan\alpha = r_1\cos\omega \quad , \quad z_s\tan\beta = r_2\cos\omega \tag{4.26}$$

Substituting the above expressions in Eq.(4.8) we get

$$r = r_1 + r_2$$

From Fig.(7a), it is seen that

$$\tan\theta_1 = \frac{r_1\cos\omega}{z_p} \quad , \quad \tan\theta_2 = \frac{r_2\cos\omega}{z_s} \tag{4.27}$$

Comparing Eq. (4.26) and (4.27), we get

$$\theta_1 = \alpha \quad \text{and} \quad \theta_2 = \beta$$

and Eq.(4.25) becomes

$$\ell_M = \sin\theta_1 = \kappa \sin\theta_2 \tag{4.28}$$

Using the above analysis, Eq.(4.24) can be written as

$$t_M = [r_1\cos\omega \sin\theta_1 + z_p\cos\theta_1] + \kappa\kappa[r_2\cos\omega \sin\theta_2 + z_s\cos\theta_2] \tag{4.29}$$

Note that this value of $t(\ell_M)$ is also a function of ω. Then

$$t_M(\omega) \geq z_p\cos\theta_1 + z_s\cos\theta_2$$

where the equality exists for $\omega=\pi/2$. t_M is a continuous function of ω ($0\leq\omega\leq\pi/2$) and from Eq.(4.4)

$$\frac{\partial t(\ell_M)}{\partial\omega} = -\ell_M r \sin\omega$$

thus, t_M is maximum for $\omega=0$. Now, Fig.(7) can be interpreted considering A as the source point, D as the receiver point and EF as a part of the surface of the half-space. In Eq.(4.28), $\sin\theta_1 = \kappa\sin\theta_2$, which is the classical law of reflection of elastic waves.

For $\omega=0$, Eq.(4.27) becomes

$$\tan\theta_1 = r_1/z_p \quad , \quad \tan\theta_2 = r_2/z_s$$

and the value of $t_M(0)$ is

$$t_M(0) = [r_1\sin\theta_1 + z_p\cos\theta_1] + \kappa[r_2\sin\theta_2 + z_s\cos\theta_2] \tag{4.30a}$$

Figure 7a. Geometric interpretation of Eq.(4.29)

Figure 7b. Geometric interpretation of Eq.(4.30a).

Note that the parameters in the above equation are non-dimensional. Restoring the dimensions according to Eq.(2.11), we find

$$t_M(0) = \frac{1}{c}(r_1 \sin\theta_1 + z_p \cos\theta_1) + \frac{1}{c_2}(r_2 \sin\theta_2 + z_s \cos\theta_2) \qquad (4.30b)$$

This is exactly the arrival time of the wave along the ray path AB as a P-wave and the path BD as a S-wave. Therefore, the value of $t=t_M$ corresponding to the stationary value $\xi=\xi_M$, is the arrival time of the ray whose path has a total vertical projection of z_p and z_s, travelling in P and S modes respectively. It is called the direct arrival time of those rays that are reflected at the surface of a half-space.

On the other hand, if the angle incidence of the S-wave is greater or equal to the critical angle, α_c where $\alpha_c = \sin^{-1}C/c$, then there will be a refracted P-wave travelling along the surface of the half-space. It means that the ray travels the path from the source to the surface in S mode and the rest in P mode. It means that, it arrives to the receiver before the direct S-wave and is called the head wave For the head waves, the slowness in the radial direction, ℓ, is equal to the slowness of the P-wave. Therefore, normalizing it with the slowness of the P-wave and considering $z_p=0$, one obtains the expression to be used in finding the arrival time of the head waves. $t_{head}|_{\omega=0} = r + z_s(\kappa^2-1)^{\frac{1}{2}}$ $\qquad (4.31)$

A third wave which is known as the Rayleigh wave exists with a velocity C_R, which is less the shear wave velocity. It is given as $C_R = 0.9194C$ [8] where C is the shear wave velocity. The Rayleigh waves decay as $r^{-\frac{1}{2}}$ in the direction of propagation and exponentially with depth. They can not be explained by a single generalized ray. The arrival time of the Rayleigh waves can be calculated for the surface and receiver case as the distance and the speed are known.

For the buried source case, the point on the surface where the Rayleigh wave originates due to diffraction is not known. Pekeris and Lifson [20] found that there were no distinct peaks in displacement for the buried source case when $r_0/z_0 < 5$.

Now consider the P and S waves travelling from a buried source to a surface receiver. For the P-wave $z_p = z_0$, $z_s = 0$ and for the S-wave $z_s = z_0$ and $z_p = 0$. Solving for the upper limit of integration, ξ_1, from Eq.(4.17), one obtains

$$\xi_1 = \frac{z_0}{r^2 + z_0^2} \sqrt{t^2 - \alpha^2(r^2 + z_0^2)} + \frac{itr}{r^2 + z_0^2} \tag{4.32}$$

where $\alpha = 1$ and κ for the P and S waves respectively.

4.4 CONVOLUTION OF RAY INTEGRALS

It was mentioned at the beginning of this chapter that the integrals of the form I_0 and I_1 appearing in the expressions of the displacements had as their coefficients, terms in the form of $s^n \bar{F}(s)$; and that the complete transient response would be given through a convolution integral involving the inverse Laplace transform of I's and their coefficients. In our study n is either 2 or 3 and the function $\bar{F}(s)$ involves the Laplace transform of the time dependency of the force input. Recalling Eq.(2.18), we have

$$s^3 \bar{F}(s) = \frac{sF_0 \bar{f}(s)}{4\pi\kappa^2 \mu r_0^2} \equiv \bar{G}_0(s)$$

$$\tag{4.33}$$

$$s^2 \bar{F}(s) = \frac{F_0 \bar{f}(s)}{4\pi\kappa^2 \mu r_0^2} \equiv \bar{G}_1(s)$$

Note that if $f(t)$ was a Heaviside's step function, $f(t)=H(t)$, then $f(s)=1/s$ and the above expressions reduce to

$$\bar{G}_0(s) = \frac{F_0}{4\pi\kappa^2\mu r_0^2}$$

$$\bar{G}_1(s) = \frac{F_0}{4\pi\kappa^2\mu r_0^2} \left(\frac{1}{s}\right) \tag{4.34}$$

Hence, the inverse Laplace transform of these quantities are

$$G_0(t) = \frac{F_0}{4\pi\kappa^2\mu r_0^2} \, \delta(t)$$

$$G_1(t) = \frac{F_0}{4\pi\kappa^2\mu r_0^2} \, H(t) \tag{4.35}$$

where $\delta(t)$ is the Delta-Dirac function. Therefore, the integrals with $s^3\bar{F}(s)$ as their coefficients should be convoluted by $\delta(t)$ and those with $s^2\bar{F}(s)$ as their coefficients should be convoluted by $H(t)$. Note that

$$\delta(t) * f(t) = \int_0^t \delta(t-\tau) \, f(\tau) \, d\tau$$

$$= f(t)$$

$$\tag{4.36}$$

$$H(t) * f(t) = \int_0^t H(t-\tau) \, f(\tau) \, d\tau$$

$$= \int_0^t f(\tau) \, d\tau$$

In view of the above relations, for a Heaviside's input, only the integrals with $s^2\bar{F}(s)$ as their coefficients should be integrated from t=0 to t=t. However, since each integral has a specific arrival time, the lower limit of integration is to be replaced by the corresponding arrival time of the ray, i.e., the integration is from t_{A_j} to t=t.

Thus using the above ideas, we take the inverse Laplace trasform of $\bar{u}_{zj}$ and $\bar{u}_{rj}$ (Eq.3.14) and get

$$u_{zj}(r,z,t) = \frac{F_0}{4\pi\kappa^2\mu r_o^2}\ (a_z I_0 + a_r I_1) \tag{4.37a}$$

$$u_{rj}\ (r,z,t) = \frac{F_0}{4\pi\kappa^2\mu r_o^2}\ [(a_z I_1 - a_r I_0)$$

$$+ \frac{a_r}{r}\ (\ \int_0^t I_1(r,z,\tau)\ d\tau + \int_0^t I_{1H}(r,z,\tau)\ d\tau)] \tag{4.37b}$$

where H denotes the SH-wave.

Note that $I_{1H}(r,z,\tau)$ can be solved analytically, yielding

$$I_{1H}(r,z,\tau) = 2\kappa \tag{4.38}$$

which agrees with the numerical results.

Chapter V

NEAR FIELD RESPONSES

In this chapter, the procedure used in calculating the ray integrals will be explained and the response of a half-space due to point, finite line and areal loads with Heaviside's step function time dependance will be discussed. Both buried and surface sources will be considered. In all the examples presented, the Poisson's ratio for the half-space material is taken as 0.25 corresponding to $\kappa^2 = 3$.

5.1 PROCEDURE IN NUMERICAL CALCULATIONS

In a half-space, waves radiated at the source location travel along different paths depending on the orientation of the source and the receiver before they reach the receiver. Therefore, as a first step in numerical calculations, a sketch of the possible wave paths should be made taking into account all the reflections, (Fig.2). Note that in all the examples presented in this work, we have taken the receiver to be on the surface of the half-space.

In the case of a buried source, the direct P-wave ($z_p = z_o$, $z_s = 0$) and the direct S-wave ($z_p = 0$, $z_s = z_o$) are the only possible waves reaching the receiver on the surface, where z_o is the depth of the source. To start the numerical calculations, the stationary point of the Cagniard's path, ξ_M, and the arrival time of the ray, t_M, are found using Eq.(4.9) and (4.10) respectively. If there is a head wave effect in the direct S-wave, the arrival time of it can be calculated from Eq.(4.31). The upper limit of integration, ξ_1, for each value of time, t, is obtained from Eq.(4.32). By choosing the appropriate source function and the receiver function, the integrands of the integrals are formed and the integration along the path $AM\xi_1$, (Fig.6),

-45-

can be carried on.

For the P-waves and the S-waves with no head wave, the stationary point ξ_M is below the point $\xi=i$. It can be shown that the integrand of the integrals are all real valued for ξ below ξ_M and since the imaginary part of the integrals are required as the answer, the response is zero for t less than t_M. This is expected because, t_M corresponding to ξ_M is the arrival time of the individual ray and no response is expected prior to the arrival of it. Hence, the path $AM\xi_1$ can be replaced by the path $QM\xi_1$ as the integral is zero along AQ. At point M, the path leaves the imaginary ξ-axis and goes along $M\xi_1$.

Now lets consider the contour $QM\xi_1P_2P_1Q$. The integrals have no singularities inside this contour. Thus, we can replace the integration along $QM\xi_1$ by the sum of the integrations along the straight lines QP_1, P_1P_2, $P_2\xi_1$, (Fig.6a). This is chosen, since it is much easier to evaluate the integrals along the straight lines. Q, P_1 and P_2 are called pivot points. The location of the pivot points were chosen as follows. Let ξ_1 be expressed as $\xi_1=a+ib$, then

If $a<0.05\ell_M$

$$Q = i0.8\ell_M$$

$$P_1 = 0.05\ell_M + i0.8\ell_M \qquad (5.1)$$

$$P_2 = 0.05\ell_M + i[0.9b + 0.1(0.8\ell_M)]$$

and if $a>0.05\ell_M$

$$Q = i0.8\ell_M$$

$$P_1 = (a + 0.03) + i0.8\ell_M \qquad (5.2)$$

$$P_2 = (a + 0.03) + i(b-0.08)$$

In the case of S-waves with the head wave effect, the stationary point M lies between the points $\xi=i$ and $\xi=i\kappa$. It can be shown that the integrals are zero for the values of ξ_1 below $\xi=i$ which

corresponds to the arrival of the head waves. (Eq.4.31). For these rays, the pivot points P_1 and P_2 are chosen as shown in Fig(6c) if ξ_1 lies on the imaginary ξ-axis and as in Fig.(6b) otherwise. Again representing ξ_1 as a+ib, the points Q, P_1 and P_2 are chosen as

If a=0, that is ξ_1 is on the imaginary ξ-axis

$Q = i0.9$

$P_1 = 0.05 + i0.9$

$P_2 = 0.05 + ib$,

$\hspace{4cm}$ (5.3)

if 0≤a<0.05

$Q = i0.9$

$P_1 = 0.05 + i0.9$

$P_2 = 0.05 + i(b-0.08)$

$\hspace{4cm}$ (5.4)

and if a>0.05

$Q = i0.9$

$P_1 = (a + 0.03) + i0.9$

$P_2 = (a + 0.03) + i(b-0.08)$

$\hspace{4cm}$ (5.5)

Note that there is a half order singularity at $\xi=\xi_1$ on the Cagniard's path due to the K function. To avoid it, a new variable, α, is introduced such that

$$\alpha = (\xi^2-\xi_1^2)^{\frac{1}{2}} , \qquad \alpha d\alpha = \xi d\xi$$

$$\alpha_{P_2} = (\xi_{P_2}^2 - \xi_1^2)^{\frac{1}{2}}$$

$\hspace{4cm}$ (5.6)

where α_{P_2} is the value of α at point P_2.

This transformation reduces the integrals of Eq.(4.23), along $P_2\xi_1$ to

$$I_0\big|_{P_2\xi_1} = H(t-t_A)\ \frac{2}{\pi}\ \mathrm{Im} \int_{\alpha_{P_2}}^{0} E_1[\xi(\alpha)]\ \frac{\alpha}{K[r,z,t;\xi(\alpha)]}\ d\alpha$$

$$(5.7)$$

$$I_1\big|_{P_2\xi_1} = -H(t-t_A)\ \frac{2}{\pi r}\ \mathrm{Im} \int_{\alpha_{P_2}}^{0} E_2[\xi(\alpha)]\ \frac{[z_p\eta(\alpha)+z_s\zeta(\alpha)-t]\ \alpha}{K[r,z,t;\xi(\alpha)]}\ d\alpha$$

When α approaches zero, the term α/K in the above integrals becomes indeterminate. To remove this, the K function is expanded into a power series around $\alpha=0$, and the common factor α is cancelled by the α in the numerator, (Appendix B).

Finally each of the integrals along QP_1, P_1P_2 and $P_2\xi_1$ in the complex ξ-plane can be transformed into an integration with respect to a real variable, y, in the interval $[-1,1]$, using the following transformations.

Along QP_1

$$\xi = \frac{1}{2}\ (\xi_{P_1} + \xi_Q) + \frac{1}{2}\ (\xi_{P_1} - \xi_Q)y$$

$$(5.8)$$

$$\frac{d\xi}{dy} = \frac{1}{2}\ (\xi_{P_1} - \xi_Q)$$

Along P_1P_2

$$\xi = \frac{1}{2}\ (\xi_{P_2} + \xi_{P_1}) + \frac{1}{2}\ (\xi_{P_2} - \xi_{P_1})y$$

$$(5.9)$$

$$\frac{d\xi}{dy} = \frac{1}{2}\ (\xi_{P_2} - \xi_{P_1})$$

Along P_1P_2

$$\alpha = (1-y)\alpha_{P_2}/2 \quad , \quad \frac{d\alpha}{dy} = -\alpha_{P_2}/2$$

$$\xi = (\alpha^2+\xi_1^2)^{\frac{1}{2}} \quad ; \quad \frac{d\xi}{d\alpha} = \alpha/\xi$$

(5.10)

Thus, Eq. (4.23) yields

$$I_0 = H(t-t_A) \frac{2}{\pi} \text{Im}[\int_{-1}^{+1} (E_1 \frac{\xi}{K} \frac{d\xi}{dy})_{QP_1} dy$$

$$+ \int_{-1}^{+1} (E_1 \frac{\xi}{K} \frac{d\xi}{dy})_{P_1P_2} dy + \int_{-1}^{+1} (E_1 \frac{\alpha}{K} \frac{d\alpha}{dy})_{P_2\xi_1} dy]$$

$$I_1 = H(t-t_A) \frac{2}{\pi r} \text{Im}[\int_{-1}^{+1} (E_2 \frac{t-z_p\eta-z_s\zeta}{K} \xi \frac{d\xi}{dy})_{QP_1} dy$$

(5.11)

$$+ \int_{-1}^{+1} (E_2 \frac{t-z_p\eta-z_s\zeta}{K} \xi \frac{d\xi}{dy})_{P_1P_2} dy$$

$$+ \int_{-1}^{+1} (E_2 \frac{t-z_p\eta-z_s\zeta}{K} \alpha \frac{d\alpha}{dy})_{P_2\xi_1} dy]$$

The above integrals can be calculated using Gaussian quadrature
integrations.

If the source is on the surface, we choose the ray groups and
the surface source functions as explained in sec.(3.5). In the
numerical calculation of the ray integrals, the procedure explained
for the buried source case is used with the following exceptions.
The integration path or the Cagniard's path lies along the imaginary

ξ-axis, and the path shown in Fig.(6c) and the pivot points given by Eq.(5.3) are used. Also, for the K function, the power series expansion is not needed, as K=rα, (Appendix B).

5.2. NUMERICAL RESULTS

5.2.1.Point Source

Since the response of a half-space due to either a buried or a surface point source has been studied in great detail [20,7,12], we present some of the results for completeness.

Numerical results for different orientations of the concentrated force are shown in Fig.(11) and (13). Note that a positive direction for the displacement is the direction of the positive z-axis which is taken into the half-space.

5.2.2.Finite Line Source

The response of a half-space due to finite sized line sources can be obtained by integrating the point source results along the line which characterizes the finite line source. Since the analytical integration is very difficult, in our work, we carry out this integration numerically. For this, the line segment is divided into n equal parts and a concentrated force is assumed to act at the middle of each segment, (Fig.9 and 10). The final solution is then obtained by summing up the responses due to each concentrated force.

Numerical results for the buried line sources are presented in Fig.(12) while those for surface line sources are shown in Fig.(14) and (15). The distances involved in such problems are all normalized with respect to the distance of the receiver from the center of the line source.
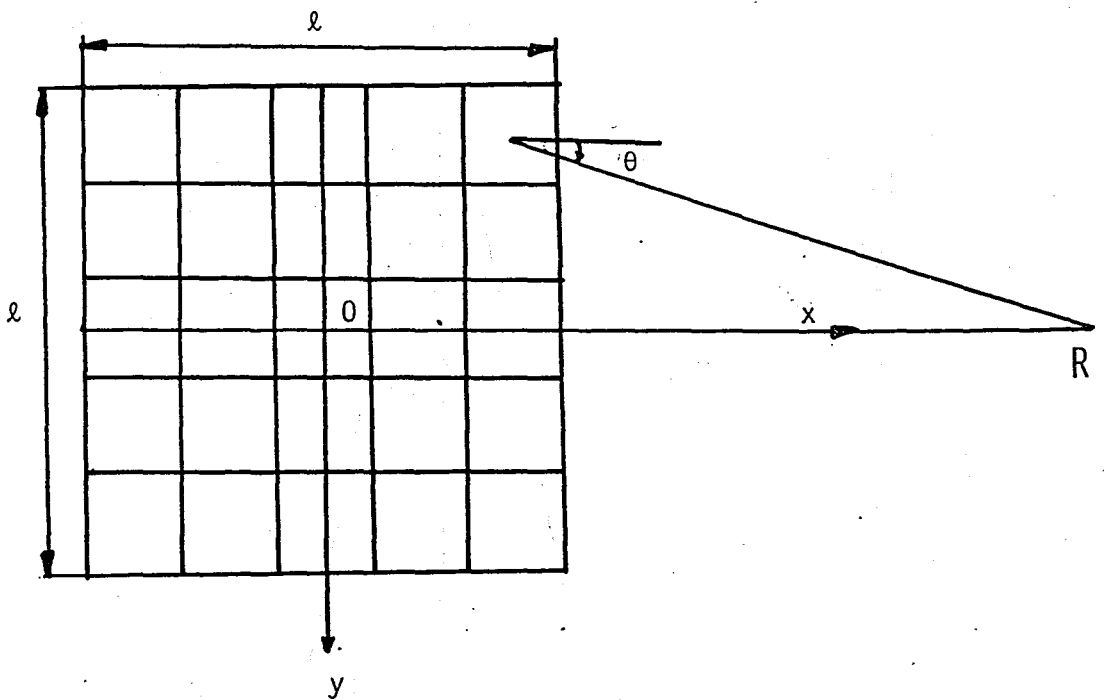
Figure 8. 5x5 point surface square area source approximation
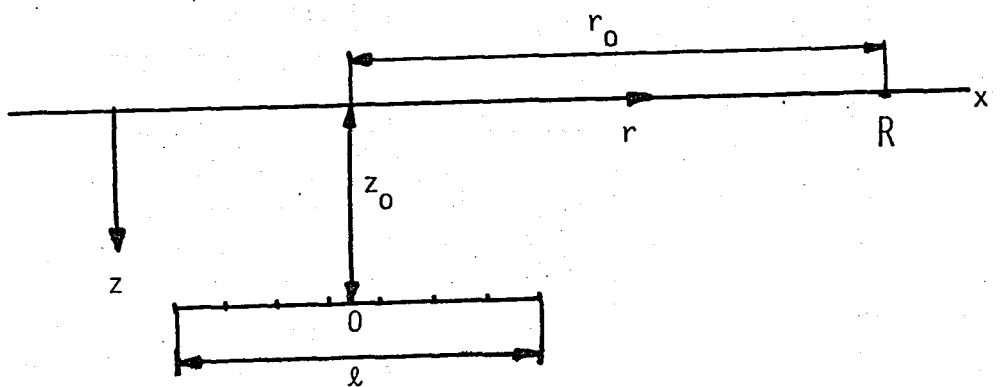
with $\ell=0.1$ and $OR=r_o=1$.

Figure 9. 7 point buried line source approximation with $\ell=0.49$,
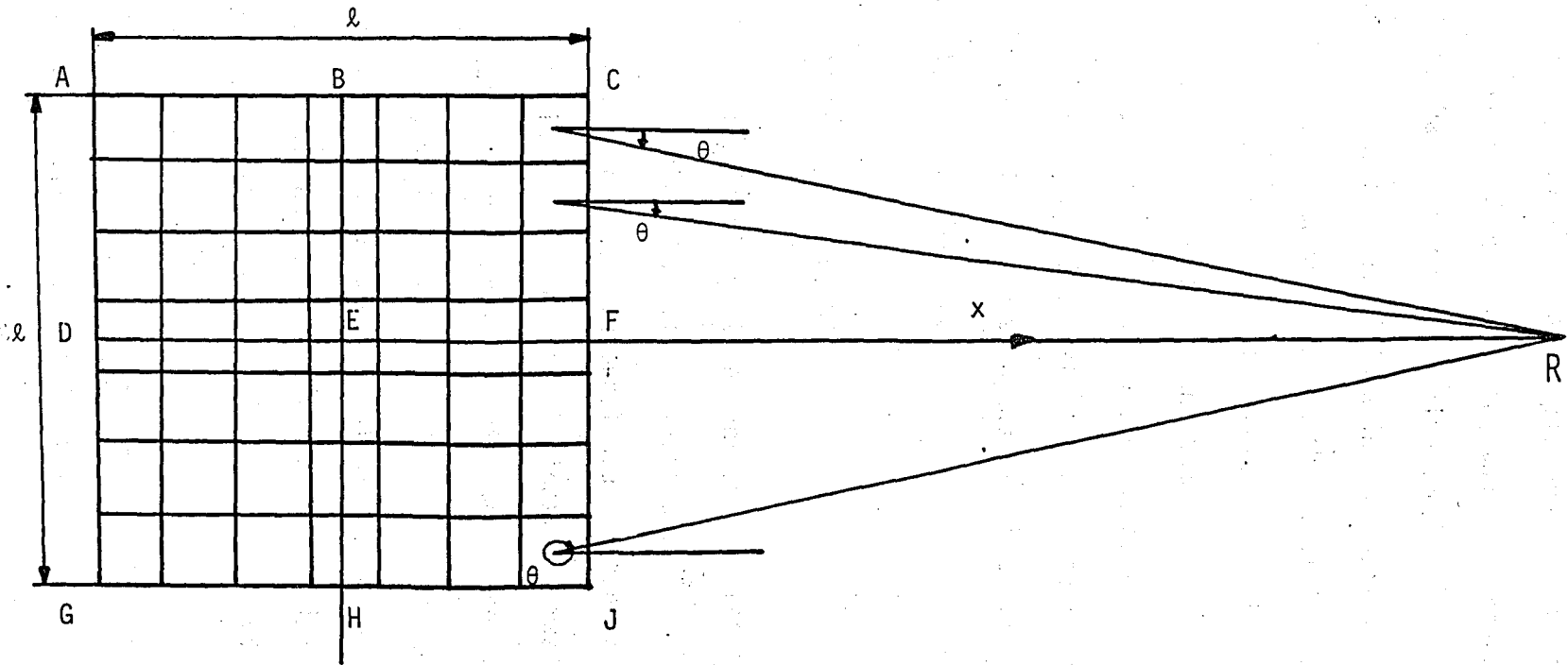
$r_o=1$ and $z_o=0.5$.

Figure 10. 7x7 point surface square area source and 7 point surface line source, BEH and DEF, approximations with $\ell=0.49$ and $ER=r_o=1$.

5.2.3. Finite Areal Source

The response of the half-space due to finite sized areal sources can be obtained by integrating the point source results over the area which characterizes the finite areal source. In the numerical integration, the area is divided into n equal subareas and a concentrated force is assumed to act at the middle of each subarea, (Fig.8 and 10). The final solution is then obtained by summing up the responses due to each concentrated force.

Numerical results for the surface areal sources are presented in Fig.(16) and (17). The distances involved in such problems are all normalized with respect to the distance of the receiver from the center of the areal source.

5.3. DISCUSSION AND CONCLUSION

The analysis of the transient surface responses of a homogeneous, isotropic and elastic half-space due to the application of a point, a finite line, and areal sources are presented in this work. Before starting the actual calculations, the results obtained from the computer program for an infinite media are compared with the corresponding analytical results given by Love [14] and Achenbach [2]. The results agreed up to 6-10 decimal points when 32 point Gaussian quadrature integration was used. Also, the analytical solution of the integral due to the SH-wave completely agrees with the numerical results (Eq.4.38).

In the following sections, the behavior of the time-displacement diagrams will be discussed for the previously described sources.

5.3.1. Buried Point Force

The numerical results for different orientations of the buried concentrated force are shown in Fig(11) for $r_0/z_0 = 2$ and $r_0 = 1$. The results agree with Pekeris and Lifson [20] for the vertical force case. In the diagrams, the finite jumps can be seen at the arrival of P and S waves. If $r_0/z_0 \geq 1/\sqrt{2}$, there is a head wave and the displacement is marked by logaritmic infinity at the arrival of it. For large ranges, $r_0/z_0 \gg 1$, it has only a sharp maximum and the solution approaches the solution of surface source [20]. A little after the arrival of S-waves, the peak due to Rayleigh waves can be seen if $r_0/z_0 \geq 5$ [20]. Note that the Green's tensor is not symmetric, which means that the vertical displacement due to a radial force is not equal to the radial displacement due to a vertical force, $u_z(a_r) \neq u_r(a_z)$.

5.3.2. Surface Point Force

The numerical results for different orientations of the surface concentrated force are shown in Fig.(13) for $r_0 = 1$. The results agree with Chao [7] for the radial force case and with Pekeris and Lifson [20] for the vertical force case. At the arrival of P and S waves, the finite jumps can be seen, and as the receiver moves away, the initial response is weaker. There is always a discontinuity at the arrival of Rayleigh waves, and the Green's tensor has the property, $u_z(a_r) = -u_r(a_z)$.

5.3.3. Buried Line Force

The numerical results for the buried line force are shown in Fig.(12) for $r_0 = 1$ and $z_0 = 0.5$. The peak due to the Rayleigh wave can not be seen as $r_0/z_0 = 2$, and it is expected to be seen for

$r_o/z_o \geq 5$ [20]. If we compare the responses of the buried point and buried line forces, they look similar, (Fig.11,12).

5.3.4. Surface Line Force

The numerical results for the surface line forces, DEF an BEH (Fig.10) are shown in Fig.(15) and (14) respectively. For the line force DEF, along the x-axis, the oscillations due to the interference of the waves from different points on the line, are seen. On the other hand, for the line force BEH, along the y-axis, waves from different points on the line interfere in such a way that the final response is very similar to that of a point force placed at the origin, (Fig.13,14). Once again, $u_z(a_r) = -u_r(a_z)$.

5.3.5. Areal Forces

The numerical results for two different surface areal forces are shown in Fig.(16) and (17). In the first, the load is taken to be distributed over a square with sides aqual to 0.1 and the distance of the receiver from the center of the load is taken as 1 (Fig.8). In the second case, the sides of the square load is taken as 0.49 while the receiver is again located at $r_o = 1$ (Fig.10). As seen, the responses in the first case are very similar to the point force case. This is expected because in the former case the ratio of the size of the load to the distance r_o of the receiver is 10 resembling the far field response while in the latter this ratio is 2 resembling the near field response of the half-space. In view of the above discussion, we can conclude that the areal forces can be resembled by point forces safely if the far field responses are in concern.

The above results can be used to explain the effect of the size of the source and the receiver, namely, the transducer used in Nondestructive Testing of materials. The numerical results show

that the fall time of the drop of the Rayleigh wave is finite for
the cases of finite line and areal sources, and zero for the case
of a point source. It is found that the responses due to areal (line)
source-point receiver and point source-areal (line) receiver cases
are equal, thus, the above analysis is valid for the receivers as
well. It is also well proven experimentally [3] that the size of
the transducer affects its accuracy. For that purpose, transducers
are calibrated by considering them as either a source or a
receiver.

In the calibration of a transducer as a receiver [10], a known
force is applied on the surface of alarge block.: and the response
obtained by a standard transducer and a test transducer are compared.
For this purpose, a transducer of known characteristics or a transfer
media of known theoretical solution is used. Note that the response ː
of a capacitive transducer agrees with the theoretical solution [10].
Simple geometries such as a large block representing a half-space
are chosen as the transfer media so that the transfer function of
it can easily be calculated. The most widely used calibration tech-
nique is the step force technique [3,10] in which the force is app-
lied by means of a breaking glass capillary or a mechanical acoustic
emission simulator.

The response of a media due to arbitrary time dependency of the
source can be obtained by applying the principle of superposition.
Mathematically, this principle can be written as [5,10]

$$h(t) = \int_{o}^{t} G(\tau)f(t-\tau)\,d\tau \qquad\qquad (5.12)$$

where G(t) is the transfer function of the media due to a $\delta(t)$ input,

f(t) is the input time function and h(t) is the output of the system. This equation can be evaluated numerically by breaking the total duration into n intervals of Δt. In matrix form it can be written as |5|

$$\frac{1}{\Delta t} \{h\} = [G] \{f\} \tag{5.13}$$

In the calibration of a transducer as a source [3], the response due to an unknown input force is picked up by a standard transducer. Then finding the transfer function of the media as explained above, the input function can be calculated by deconvoluting Eq.(5.12). In matrix from, using Eq.(5.13), it can be written as

$$\{f\} = \frac{1}{\Delta t} [G]^{-1} \{h\} \tag{5.14}$$

Thus, in this work, we obtained the theoretical solution for an isotropic, homogeneous and elastic half-space due to the application of a point, a finite line and areal sources with a Heaviside's step input function. The solutions can be used as a comparison in the calibration of transducers having different sizes. In the future, a layered media can be studied in detail, by applying the afore-mentioned sources; and the effect of the size and the location of the source and the receiver can be analyzied.

REFERENCES

[1] Abromovitz, M. and Stegun, I.A., Handbook of Mathematical Functions, U.S. Government Printing Office, Washington, D.C., 1964.

[2] Achenbach, J.D., Wave Propagation in Elastic Solids, North-Holland Company, London; 1973.

[3] Breckenridge, F.R., Tschiegg, C.E. and Greenspan, M., "Acoustic Emission: Some Application of Lambs Problem", J.Acoust. Soc. Am. 57, P.626, 1975.

[4] Cagniard, L., "Reflection and Refraction of Progressive Seismic Waves", Translated by Flynn, E.A. and Dix, C.H., Mc Graw-Hill Book Co., NewYork, 1962.

[5] Ceranqglu, A., Acoustic Emission and Propagation of Elastic Pulses in a Plate, Ph.D.Thesis, Cornell University, Ithaca, NewYork, 1979.

[6] Chandra,V., "Theory of Head Waves for Focal Mechanism Studies", Bull. Seism. Soc.Am., 58, p.993, 1968.

[7] Chao, C.C., "Dynamical Response of an Elastic Half-Space to Tangential Surface Loadings", J.Appl. Mechanics, 27, p.539, 1960.

[8] Ewing, W.M., Jardetzky, W.S. and Press, F., Elastic Waves in Layered Media, Mc Graw-Hill Book Co., NewYork, 1957.

[9] Garvin, W.W., "Exact Transient Solution of the Buried Line Source Problem", Proc. of the Royal Soc., London, Ser. A, p.234, 1956.

[10] Hsü, N.N. and Breckenridge, F.R., "Characterization and Calibration of Acoustic Emission Sensors", Materials Evaluation, 39, p.60, Jan.1981.

[11] Knopoff, L. and Gilbert, F., "First Motions from Seismic Sources", Bull. Seism. Soc.Am,, 50, p.117, 1960.

[12] Lamb, H., "On the Propagation of Tremors Over the Surface of an Elastic Solid", Phil. Transactions of Royal So. of London, Ser. A, 242, p.63, 1904.

[13] Lapwood, E.R., "The Distrubance due to a Line Source in a Semi Infinite Elastic Medium", Phil. Trans. of Royal Soc. of London, Ser. A, 242, p.63, 1949.

[14] Love, A.E.H., A Treatise on the Mathematical Theory of Elasticity, Dover, NewYork, 1944.

[15] Morse, P.M. and Feshbach, H., Methods of Theoretical Physics, Mc.Graw-Hill, NewYork, V. 1; 1953.

[16] Norwood, F.R., "Exact Transient Response of an Elastic Half-Space Loaded Over a Rectangular Region of Its Surface", J. of Appl. Mechanics., p.516, Sep.1969.

[17] Norwood, F.R., "Response of an Elastic Half-Space to Impulsive Stationary Finite Line Sources", J. of Appl. Mech., p.549, June, 1971.

[18] Norwood, F.R., "Transient Response of an Elastic Plate to Loads with Finite Characteristic Dimensions", Int. J. Solids and Structures, 11, p.33, 1975.

[19] Pao, Y.H. and Gajewski, R., "The Generalized Ray Theory and Transient Response of Layered Elastic Solids", Physical Acoustics, 13, Ch.6, 1977.

[20] Pekeris, C.L. and Lifson, H., "Motion of the Surface of a Uniform Elastic Half-Space Produced by a Buried Pulse", J. Acoust. Soc. Am., p.1233, 1957,

[21] Sherwood, J.W.C., "Transient Sound Propagation in a Layered Liquid Medium", J.Acoust. Soc. Am., 32, p.1673, 1960.

[22] Spencer, T.W., "The Method of Generalized Reflection and Transmission Coefficients", Geopysics, 25, p.625. 1960.

[23] Sternberg, E., "On the Integration of the Equation of Motion in the Classical Theory of Elasticity", Archiv. for Rational Mechanics and Analysis, 6, p.34, 1960.

[24] Wu, J.H., Transient Analysis of a Three-Dimensional Elastic Plate by the Ray Grouping Technique, Ph.D. Thesis, University of New-Mexico, 1975.

DISPLACEMENT POTENTIALS FOR AN ARBITRARILY ORIENTED
CONCENTRATED FORCE IN AN UNBOUNDED MEDIUM

In this appendix, a detailed derivation of the displacement potentials of Eq.(2.17) will be presented using an approach given by Achenbach [2].

For an elastic, isotropic and homogenous medium, the displacement field, $\underset{\sim}{u}$, satisfies the equation.

$$\mu\nabla^2\underset{\sim}{u} + (\lambda+\mu)\underset{\sim}{\nabla}\nabla\cdot\underset{\sim}{u} + \rho\underset{\sim}{F} = \rho\underset{\sim}{\ddot{u}} \tag{A.1}$$

Note that the parameters were previously defined in sec.(2.1).

Consider a concentrated force of magnitude $f(t)$, directed along the constant unit vector $\underset{\sim}{a}$, and acting at the point $\underset{\sim}{x}_0$ in the cartesian coordinate system, (Fig.1). Thus, the force is represented by

$$\underset{\sim}{F}(\underset{\sim}{x},t) = \underset{\sim}{a}f(t)\,\delta(\underset{\sim}{x}-\underset{\sim}{x}_0) \tag{A.2}$$

where $\delta(\underset{\sim}{x}-\underset{\sim}{x}_0)$ is Delta-Dirac function. Now, we wish to decompose Eq.(A.1) using Eq.(2.5). The result of the decomposition is

$$c^2\nabla^2\phi + G = \ddot{\phi} \tag{2.6}$$

$$c^2\nabla^2\underset{\sim}{\psi}_1 + \underset{\sim}{H} = \underset{\sim}{\ddot{\psi}}_1$$

If $\underset{\sim}{F}(x,t)$ is given, G and $\underset{\sim}{H}$ can be found. Consider the equation

$$\nabla^2\underset{\sim}{W} = \underset{\sim}{F} \tag{A.3}$$

which is known as the vector Poisson's [15] equation. Solving for $\underset{\sim}{W}$, we have [2]

$$\underset{\sim}{W} = \frac{-1}{4\pi} \int_V \frac{\underset{\sim}{F}(\underset{\sim}{x}')}{|\underset{\sim}{x}-\underset{\sim}{x}'|} d\underset{\sim}{x}' \tag{A.4}$$

where V is the volume of the body. Using the identity

$$\nabla^2 \underset{\sim}{W} = \underset{\sim}{\nabla}(\underset{\sim}{\nabla}\cdot\underset{\sim}{W}) - \underset{\sim}{\nabla}\times(\underset{\sim}{\nabla}\times\underset{\sim}{W}) \tag{A.5}$$

in Eq.(A.3) and comparing the result with Eq.(2.5), we get

$$G = \underset{\sim}{\nabla}\cdot\underset{\sim}{W} \quad , \quad \underset{\sim}{H} = -\underset{\sim}{\nabla}\times\underset{\sim}{W} \tag{A.6}$$

Hence, considering Eq.(A.2) and (A.6), Eq.(2.6) can be written as

$$c^2\nabla^2\phi - \frac{f(t)}{4\pi} \underset{\sim}{\nabla}\cdot(\frac{\underset{\sim}{a}}{R}) = \ddot{\phi} \tag{A.7}$$

$$c^2\nabla^2\underset{\sim}{\psi}_1 + \frac{f(t)}{4\pi} \underset{\sim}{\nabla}\times(\frac{\underset{\sim}{a}}{R}) = \ddot{\underset{\sim}{\psi}}_1$$

where $R^2 = (x-x_0)^2 + (y-y_0)^2 + (z-z_0)^2$

Now, introducing the following non-dimensional quantities

$$\hat{\phi} = \phi r_0^{-2} \quad , \quad \hat{R} = R/r_0 \quad , \quad \hat{\underset{\sim}{\nabla}} = r_0\underset{\sim}{\nabla} \tag{A.8}$$

$$\hat{\underset{\sim}{\psi}}_1 = \underset{\sim}{\psi}_1 r_0^{-2} \quad , \quad \kappa = c/C \quad , \quad \hat{t} = tc/r_0$$

Eq.(A.7) yields

$$\hat{\nabla}^2\hat{\phi} - f_1(t)\hat{\underset{\sim}{\nabla}}\cdot(\frac{\underset{\sim}{a}}{\hat{R}}) = \ddot{\hat{\phi}}$$

$$\hat{\nabla}^2\hat{\psi}_1 + \kappa^2 f_1(t)\hat{\underset{\sim}{\nabla}}\times (\frac{\underset{\sim}{a}}{\hat{R}}) = \kappa^2\ddot{\hat{\psi}}_1 \tag{A.9}$$

$$f_1(t) = \frac{f(t)}{4\pi c^2 r_o^2}$$

where r_o is the radial distance from the source to the receiver. Dropping the "hat", and taking Laplace transform after introducing

$$\phi = \underset{\sim}{\nabla}\cdot(\underset{\sim}{a}\phi)$$

$$\underset{\sim}{\psi}_1 = \underset{\sim}{\nabla}\times(\underset{\sim}{a}\Psi) \tag{A.10}$$

Eq.(A.9) becomes

$$\nabla^2\bar{\Phi} - \bar{f}_1(s)\frac{1}{R} = s^2\bar{\Phi}$$

$$\nabla^2\bar{\Psi} - \bar{f}_1(s)\frac{1}{R} = s^2\kappa^2\bar{\Psi} \tag{A.11}$$

where $\bar{\underset{\sim}{\Phi}}(\underset{\sim}{x},s) = \int_o^\infty \Phi(\underset{\sim}{x},t)e^{-st}\,dt$

Since the inhomogeneous terms in Eq.(A.11) show polar symmetry, it is easier to obtain the solution using spherical coordinates. Thus, Eq.(A.11) can be written as

$$\frac{1}{R^2} \frac{\partial}{\partial R} \left(R^2 \frac{\partial \bar{\Phi}}{\partial R} \right) - \bar{f}_1(s) \frac{1}{R} = s^2 \bar{\Phi} \qquad (A.12)$$

Introducing $\bar{\Phi} = \bar{\Phi}_1/R$ $\qquad\qquad$ (A.13)

we get

$$\frac{d^2 \bar{\Phi}_1}{dR^2} - s^2 \bar{\Phi}_1 = \bar{f}_1(s) \qquad (A.14)$$

with the boundary condition that $\bar{\Phi}$ has to be finite at the origin, $R = 0$. Therefore

$$\bar{\Phi}(R,s) = \frac{\bar{f}_1(s)}{s^2 R} (e^{-sR} - 1) \qquad (A.15a)$$

and similarly

$$\bar{\Psi}(R,s) = \frac{\bar{f}_1(s)}{s^2 R} (e^{-s\kappa R} - 1) \qquad (A.15b)$$

At this step, taking Laplace transform of Eq.(2.5) and (A.10), we get

$$\underset{\sim}{\bar{u}} = \underset{\sim}{\nabla} \bar{\phi} + \underset{\sim}{\nabla} \times \underset{\sim}{\bar{\psi}}_1$$

$$\bar{\phi} = \underset{\sim}{\nabla} \cdot (\underset{\sim}{a} \bar{\Phi}) \qquad (A.16)$$

$$\underset{\sim}{\bar{\psi}}_1 = -\underset{\sim}{\nabla} \times (\underset{\sim}{a} \bar{\Psi})$$

Thus

$$\underset{\sim}{\bar{u}} = \underset{\sim}{\nabla}(\underset{\sim}{\nabla}.a\bar{\Phi}) - \underset{\sim}{\nabla}x(\underset{\sim}{\nabla}xa\bar{\Psi})$$

$$= \underset{\sim}{\nabla}(\underset{\sim}{\nabla}\cdot a\bar{\Phi}) - \underset{\sim}{\nabla}(\underset{\sim}{\nabla}\cdot a\bar{\Psi}) + \underset{\sim}{a}\nabla^2\bar{\Psi}$$

$$= \underset{\sim\sim}{\nabla\nabla}\cdot\underset{\sim}{a}(\bar{\Phi}-\bar{\Psi}) + \underset{\sim}{a}(\kappa^2 s^2\bar{\Psi} + \kappa^2\bar{f}_1(s)/R)$$

Substituting the expressions for $\bar{\Phi}$ and $\bar{\Psi}$ from Eq.(A.15), the above equation yields

$$\underset{\sim}{\bar{u}} = \frac{\bar{f}_1(s)}{s^2}[\underset{\sim\sim}{\nabla a}\cdot\underset{\sim}{\nabla}(g_p-g_s) + \underset{\sim}{a}\kappa^2 s^2 g_s] \tag{A.17}$$

where

$$g_p = \frac{e^{-sR}}{R} \quad , \quad g_s = \frac{e^{-s\kappa R}}{R} \tag{A.18}$$

Note that R is given by Eq.(A.7). Also note that Eq.(A.17) agrees with Pao and Gajewski [19]. The functions g_p and g_s are called the radial wawe functions for longitudinal and shear wawes. Using Sommerfield's integral representation [8], g_p and g_s can also be written as

$$g_p = \frac{e^{-sR}}{R} = s\int_0^\infty \frac{\xi}{\eta} e^{-s\eta|z-z_0|}J_0(s\xi r)\ d\xi$$

$$\tag{A.19}$$

$$g_s = \frac{e^{-s\kappa R}}{R} = s\int_0^\infty \frac{\xi}{\zeta} e^{-s\zeta|z-z_0|}J_0(s\xi r)\ d\xi$$

where

$$\eta = (\xi^2 + 1)^{\frac{1}{2}} \quad , \quad \zeta = (\xi^2 + \kappa^2)^{\frac{1}{2}}$$

$$\text{(A.20)}$$

$$r^2 = (x - x_0)^2 + (y - y_0)^2$$

From Eq.(A.17), we can obtain the components of the displacement, $\bar{u}$, as follows

$$\bar{u}_r(r,s) = \frac{\bar{f}_1(s)}{s^2}[(a_r \frac{\partial^2}{\partial r^2} + a_z \frac{\partial^2}{\partial r \partial z})(g_p - g_s) + a_r s^2 \kappa^2 g_s]$$

$$\bar{u}_\theta(r,s) = \frac{\bar{f}_1(s)}{s^2} a_\theta [\frac{\partial}{\partial r}(g_p - g_s) + s^2 \kappa^2 g_s] \qquad \text{(A.21)}$$

$$\bar{u}_z(r,s) = \frac{\bar{f}_1(s)}{s^2}[(a_r \frac{\partial^2}{\partial r \partial z} + a_z \frac{\partial^2}{\partial z^2})(g_p - g_s) + a_z s^2 \kappa^2 g_s]$$

Note that the term $\bar{f}_1(s)/s^2 R$ in Eq.(A.15) does not appear in the expressions for the displacements, so it also won't be seen in the stress expressions. Dropping this term and using Eq.(A.19), we get

$$\bar{\Phi}(r,s) = \frac{\bar{f}_1(s)}{s} \int_0^\infty \frac{\xi}{\eta} e^{-s\eta|z-z_0|} J_0(s\xi r) \, d\xi$$

$$\text{(A.22)}$$

$$\bar{\Psi}(r,s) = \frac{\bar{f}_1(s)}{s} \int_0^\infty \frac{\xi}{\zeta} e^{-s\zeta|z-z_0|} J_0(s\xi r) \, d\xi$$

The relations between the potentials and the displacements are given by Eq.(2.19). Using those and Eq.(A.21), the expressions for the potentials $\bar{\psi}$ and $\bar{\chi}$ are obtained as [19].

$$\bar{\psi} = -a_z \frac{\bar{f}_1(s)}{s} \int_0^\infty S_v e^{-s\zeta|z-z_0|} J_0(s\xi r)\, d\xi$$

$$-a_r \frac{\bar{f}_1(s)}{s} \int_0^\infty S_v' e^{-s\zeta|z-z_0|} J_1(s\xi r)\, d\xi \tag{A.23}$$

$$\bar{\chi} = -a_\theta \bar{f}(s) \int_0^\infty S_H e^{-s\zeta|z-z_0|} J_1(s\xi r)\, d\xi$$

and, using Eq.(A.10) and (A.22), we get the potential $\bar{\phi}$ as [19]

$$\bar{\phi} = \underset{\sim}{\nabla} \cdot (\underset{\sim}{a}\bar{\Phi})$$

$$= \bar{f}_1(s) a_z \int_0^\infty S_p e^{-s\eta|z-z_0|} J_0(s\xi r)\, \xi\, d\xi \tag{A.24}$$

$$+\bar{f}_1(s) a_r \int_0^\infty S_p' e^{-s\eta|z-z_0|} J_1(s\xi r)\, \xi\, d\xi$$

where ε is the directivity parameter

$$\varepsilon = \mathrm{sgn}(z-z_0) \quad , \quad \bar{f}_1(s) = \bar{f}(s)/4\pi r_0^2 c^2 \quad , \quad S_H = \kappa^2/\zeta$$

$$\tag{A.25}$$

$$S_p = -\varepsilon \quad , \quad S_p' = -\xi/\eta \quad ; \quad S_v = \xi/\zeta \quad , \quad S_v' = \varepsilon$$

APPENDIX B

THE POWER SERIES EXPANSION OF THE "K" FUNCTION

In the discussion of sec.(5.1), it was said that the path of integration has a singularity at the upper limit of integration, ξ_1. The singularity occurs, when ξ approaches ξ_1, due to the K function given by Eq.(4.22) as

$$\frac{\xi}{K(r,z,t;\xi)} = \frac{\xi}{[\xi^2 r^2 + (z_p \eta + z_s \zeta - t)^2]^{\frac{1}{2}}} \tag{B.1}$$

To remove the singularity, a new variable α, given by Eq.(5.6), is introduced as

$$\xi^2 = (\alpha^2 + \xi_1^2)^{\frac{1}{2}} \tag{B.2}$$

Thus, we get

$$\frac{\xi}{K(r,z,t;\xi)} = \frac{\alpha}{K(r,z,t;\xi(\alpha))} \tag{B.3}$$

The above equation is undeterminate when α approaches zero. To remove it, the K function will be expanded into a power series around $\alpha=0$. Note that Eq.(B.1) can also be written as

$$\frac{\xi}{K} = \frac{\xi}{[(i\xi r + z_p \eta + z_s \zeta - t)(-i\xi r + z_p \eta + z_s \zeta - t)]^{\frac{1}{2}}} \tag{B-4}$$

It is understood that the undeterminancy occurs due to the second

-67-

bracket in the denominator, for, from Eq.(4.17)

$$t = -i\xi_1 r + z_p \eta_1 + z_s \zeta_1 \qquad\qquad (4.17)$$

Thus, only that bracket will be expanded into a power series. Using Eq.(B.2), we have

$$-i\xi r + z_p \eta + z_s \zeta - t = -ir(\alpha^2 + \xi_1^2)^{\frac{1}{2}} + z_p(\alpha^2 + \xi_1^2 + 1)^{\frac{1}{2}}$$

$$+ z_s(\alpha^2 + \xi_1^2 + \kappa^2)^{\frac{1}{2}} - t \qquad\qquad (B.5)$$

Then consider the following definition of power series expansion around $\alpha = 0$

$$(\alpha^2 + L^2) \doteq L + \frac{1}{2}\frac{\alpha^2}{L} - \frac{1}{8}\frac{\alpha^4}{L^3} + \frac{1}{16}\frac{\alpha^6}{L^5} - \frac{5}{128}\frac{\alpha^8}{L^7} + \frac{7}{256}\frac{\alpha^{10}}{L^9} - \frac{21}{1024}\frac{\alpha^{12}}{L^{11}} + ..$$

$$(B.6)$$

To apply the above expansion in Eq.(B.5), take, $L = \xi_1$ for the first bracket, $L = \eta_1$ for the second and $L = \zeta_1$ for the third, where

$$\eta_1 = (\xi_1^2 + 1)^{\frac{1}{2}} \qquad , \qquad \zeta_1 = (\xi_1^2 + \kappa^2)^{\frac{1}{2}}$$

Considering these values, we get

$$K(r,z,t;\xi(\alpha)) = \{[ir(\alpha^2 + \xi_1^2)^{\frac{1}{2}} + z_p(\alpha^2 + \xi_1^2 + 1)^{\frac{1}{2}} + z_s(\alpha^2 + \xi_1^2 + \kappa^2)^{\frac{1}{2}} - t]\alpha^2$$

$$[-ir(\frac{1}{2\xi_1} - \frac{1}{8}\frac{\alpha^2}{\xi_1^3} + ...) + z_p(\frac{1}{2\eta_1} - \frac{1}{8}\frac{\alpha^2}{\eta_1^3} + ...)$$

$$+ z_s(\frac{1}{2\zeta_1} - \frac{1}{8}\frac{\alpha^2}{\zeta_1^3} + ...) - t]\}^{\frac{1}{2}} \qquad\qquad (B.7)$$

Finally, substituting the above equation in Eq.(B.3), α's are cancelled and the uncertainty is removed.

The above expansion is needed for the buried source problem. For the surface source case, the expression for the K function can easily be found. For this case, $z_o = 0$, thus, $z_p = z_s = 0$. Substituting those in Eg.(B.1)

$$\frac{\xi}{K(r,z,t;\xi)} = \frac{\xi}{(\xi^2 r^2 + t^2)^{\frac{1}{2}}} \tag{B.8}$$

and using Eq.(B.2), we get

$$\frac{\alpha}{K(r,z,t;\xi(\alpha))} = \frac{\alpha}{(\alpha^2 r^2 + \xi_1^2 r^2 + t^2)^{\frac{1}{2}}} \tag{B.9}$$

Now, reconsider $z_p = z_s = 0$, then Eq.(4.17) yields

$$t = -i\xi_1 r \tag{B.10}$$

Thus, Eq.(B.9) becomes

$$\frac{\alpha}{K} = \frac{1}{r} \qquad \text{or} \qquad K = \alpha r \tag{B.11}$$

SOURCE AND RECEIVER FUNCTIONS FOR THE SINGLE FORCE

1) Interior Source Functions

$$S_p = -\varepsilon$$

$$S_p' = -\xi/\eta$$

$$S_v = \xi/\zeta$$

$$S_v' = \varepsilon$$

$$S_H = \kappa^2/\zeta$$

2) Surface Source Functions

$$S_p = \Omega 2\kappa^2(\xi^2+\zeta^2)/\Delta r$$

$$S_p' = 4\kappa^2\xi\zeta/\Delta r$$

$$S_v = -4\kappa^2\eta\xi/\Delta r$$

$$S_v' = -\Omega 2\kappa^2(\xi^2+\zeta^2)/\Delta r$$

$$S_H = 2\kappa^2/\zeta$$

3) Interior Receiver Functions

$$D_{zp} = -\varepsilon\eta$$

$$D_{zv} = -\xi$$

$$Drp = D_{\theta p} = -\xi$$

$$D_{rv} = D_{\theta v} = -\varepsilon\zeta$$

$$D_{rH} = D_{\theta H} = 1$$

4) Surface Receiver Functions

$$D_{zp} = -2\kappa^2\Omega\eta(\xi^2+\zeta^2)/\Delta r$$

$$D_{zv} = 4\kappa^2\eta\zeta\xi/\Delta r$$

$$D_{rp} = D_{\theta p} = 4\kappa^2\zeta\eta\xi/\Delta r$$

$$D_{rv} = D_{\theta v} = -2\kappa^2\Omega\zeta(\xi^2+\zeta^2)/\Delta r$$

$$D_{rH} = D_{\theta H} = 2$$

where

$$\Delta r = 4\xi^2 \eta \zeta - (\xi^2 + \zeta^2)^2$$

Note that if the vertical projection of a ray is in the positive z-direction, $\varepsilon = +1$; if not, $\varepsilon = -1$. At the surface of a half-space, where z=0, $\Omega = +1$.
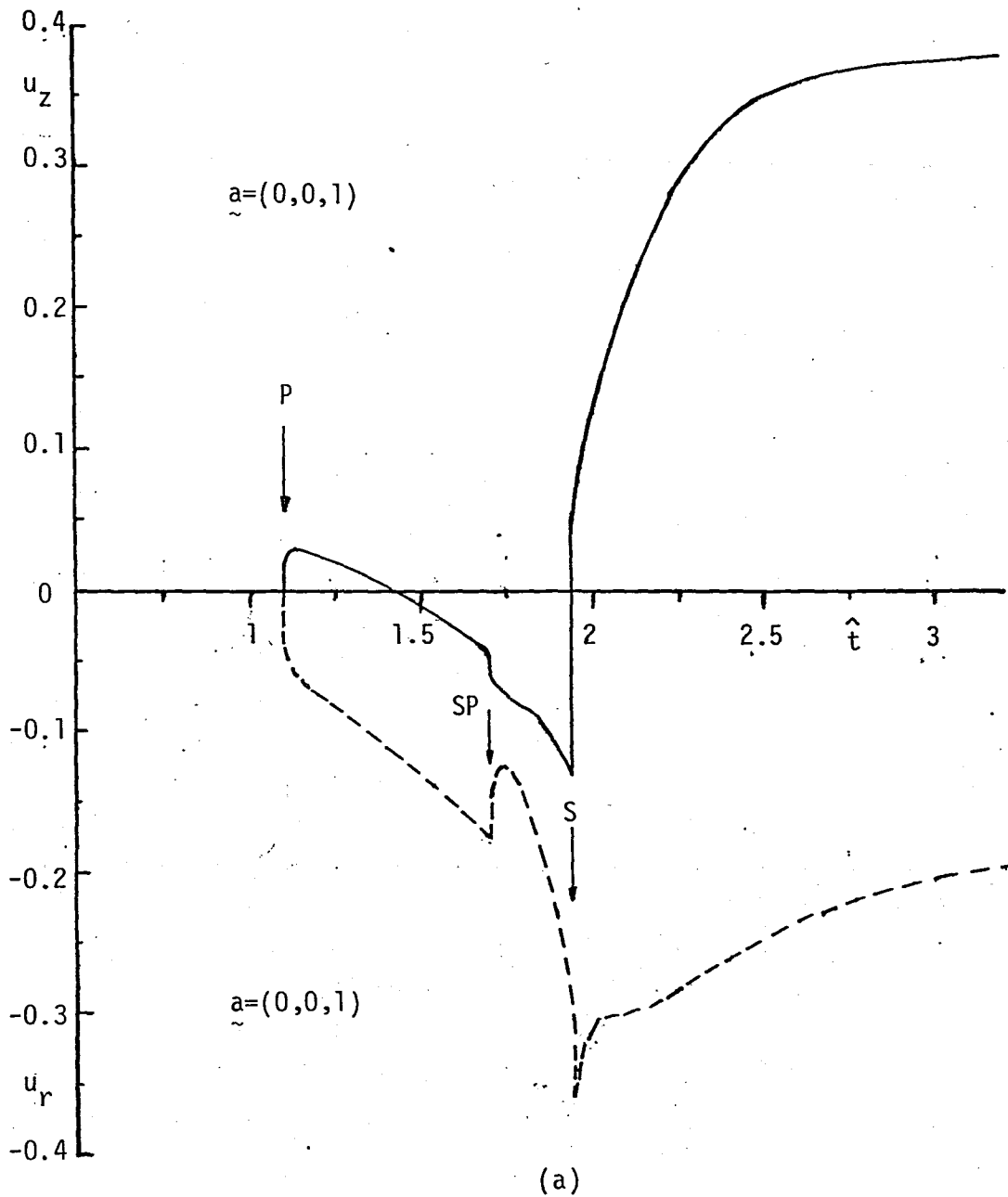
Figure 11. Response due to a buried point source. The ordinate

is the normalized nondimensional displacement

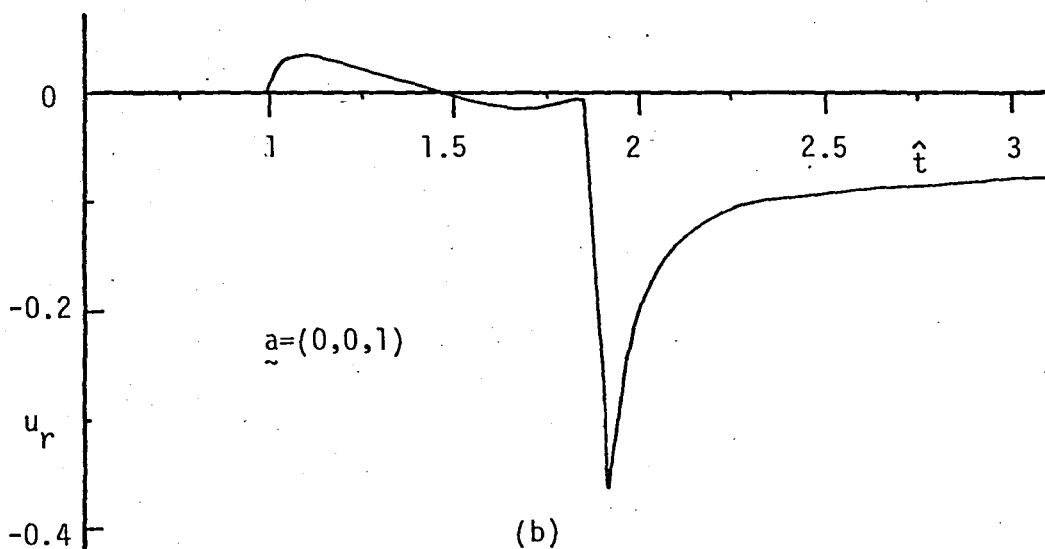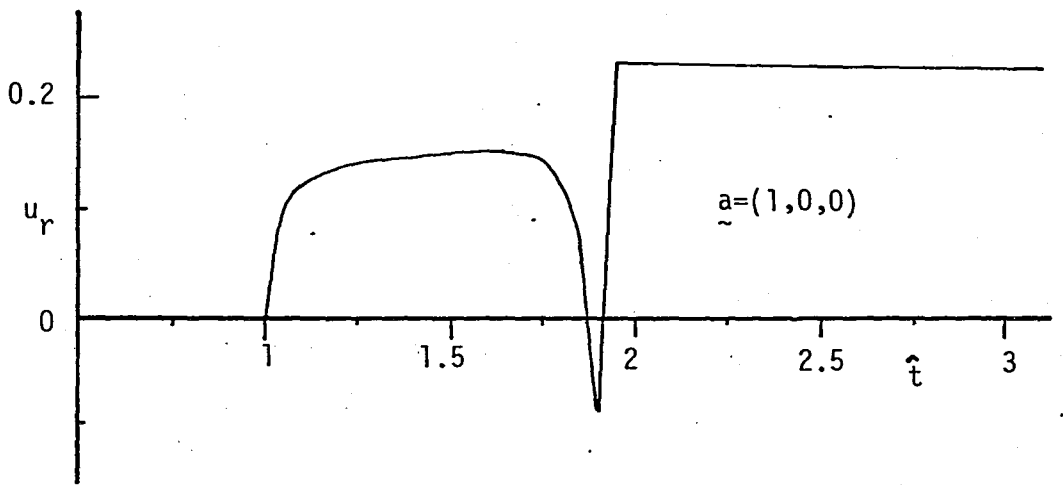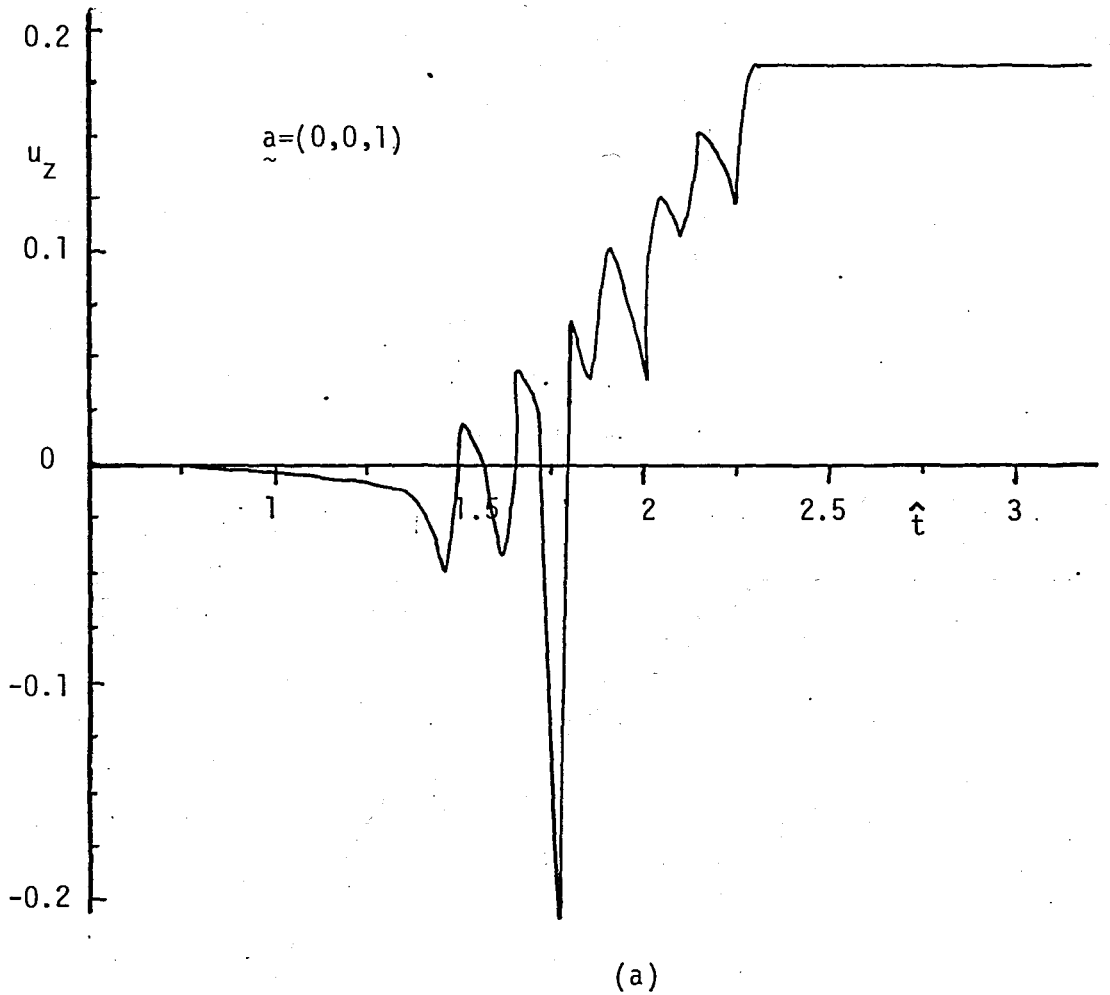$u=u\pi\mu r_0^2/F_0$ and $\hat{t}=tc/r_0$ with $r_0=1$ and $z_0=0.5$.
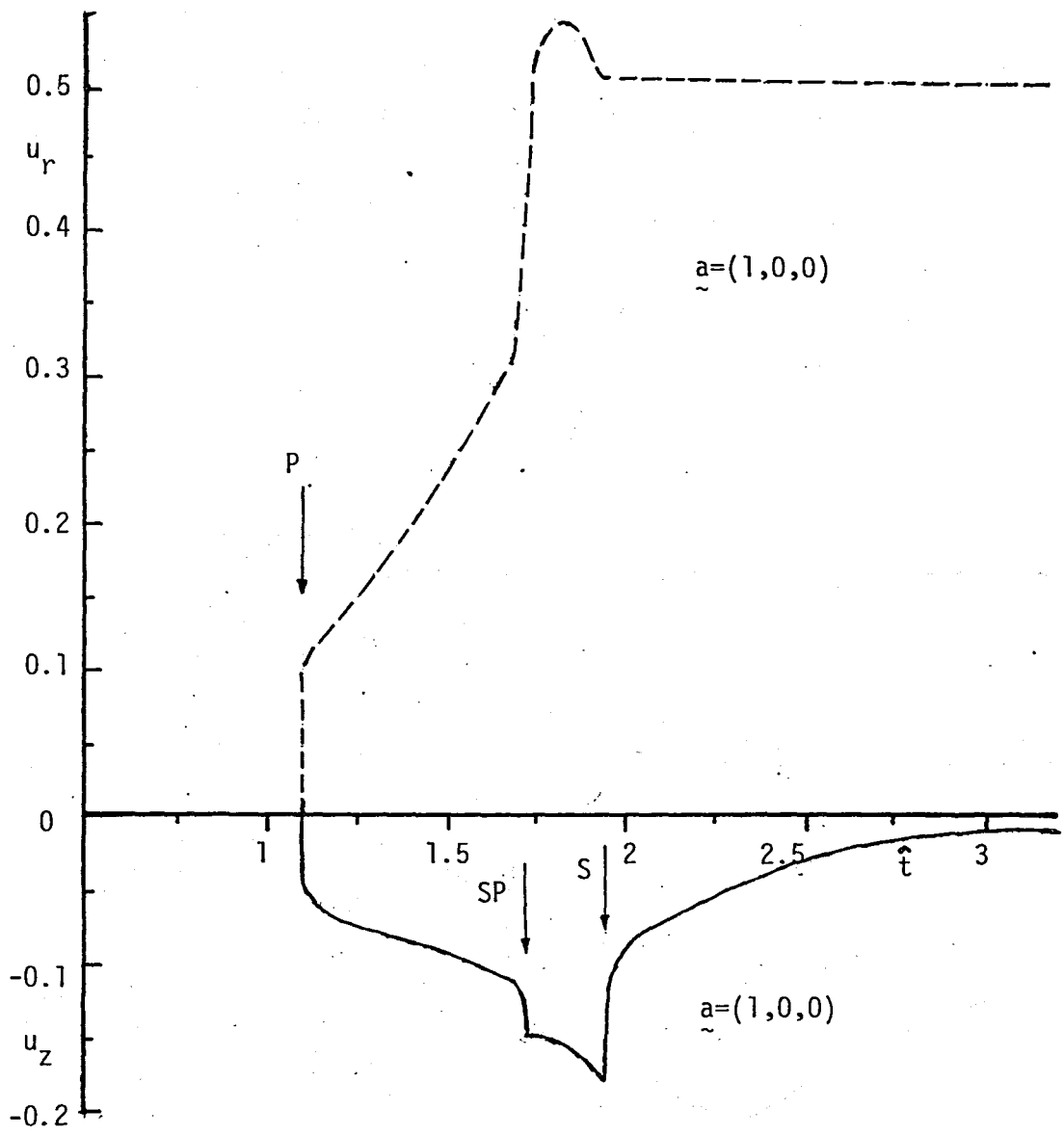
Figure 11b.
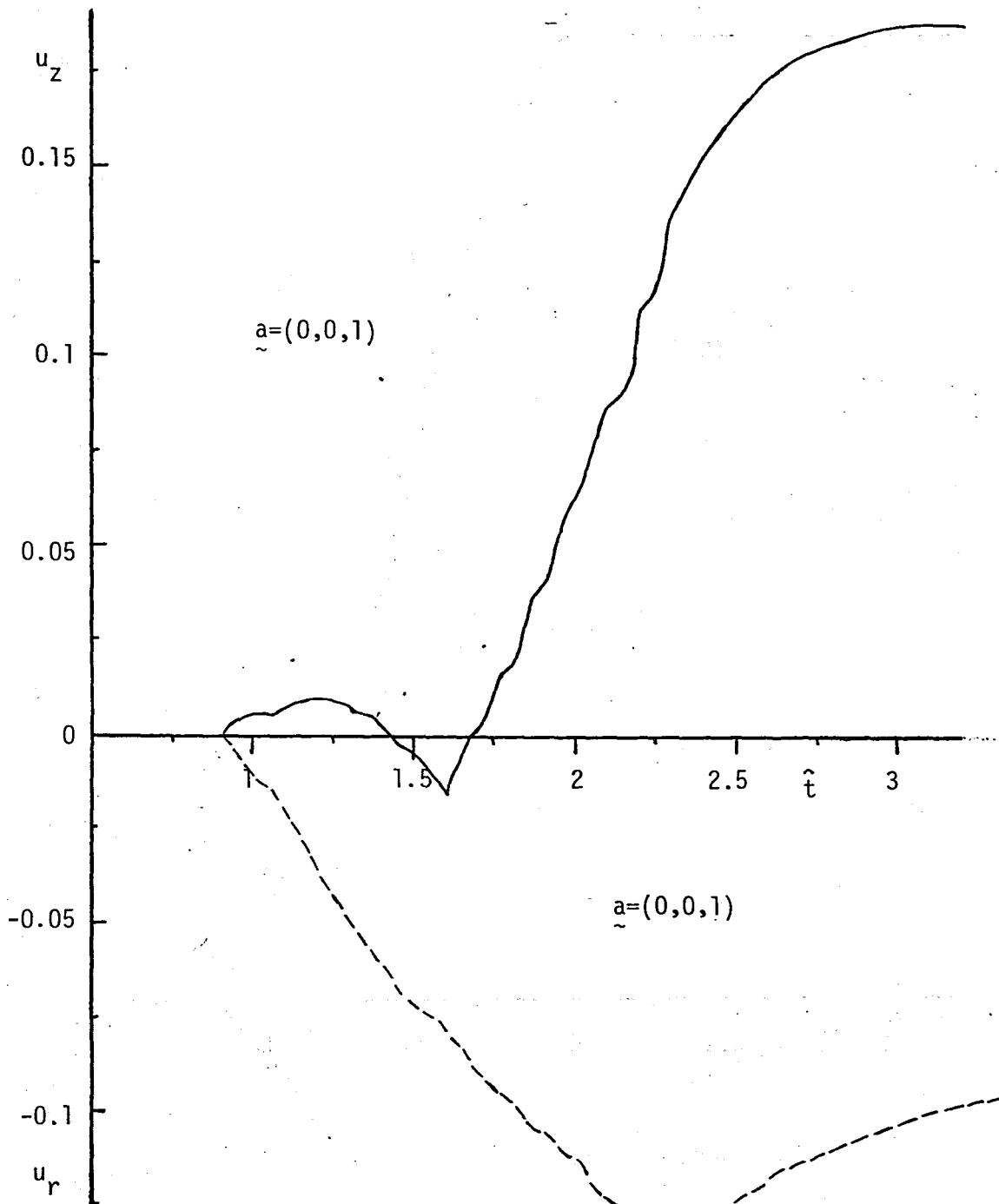
(a)

Figure 12. Response due to a buried line source. The ordinate is
is the normalized nondimensional displacement
$u = u\pi\mu r_o^2/F_o$ and $\hat{t} = tc/r_o$ with $r_o = 1$, $z_o = 0.5$ and $\ell = 0.49$.
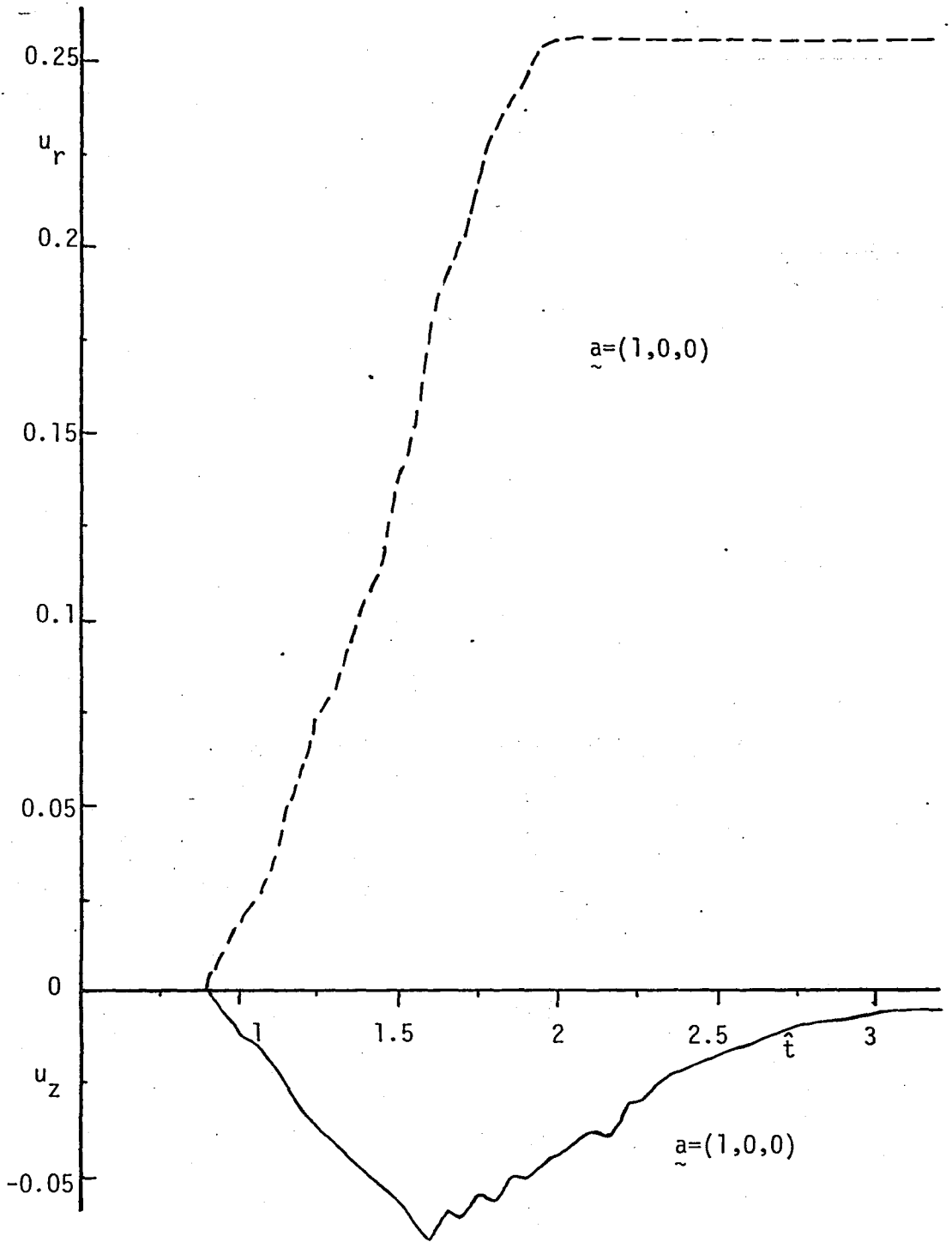
Figure 12b.
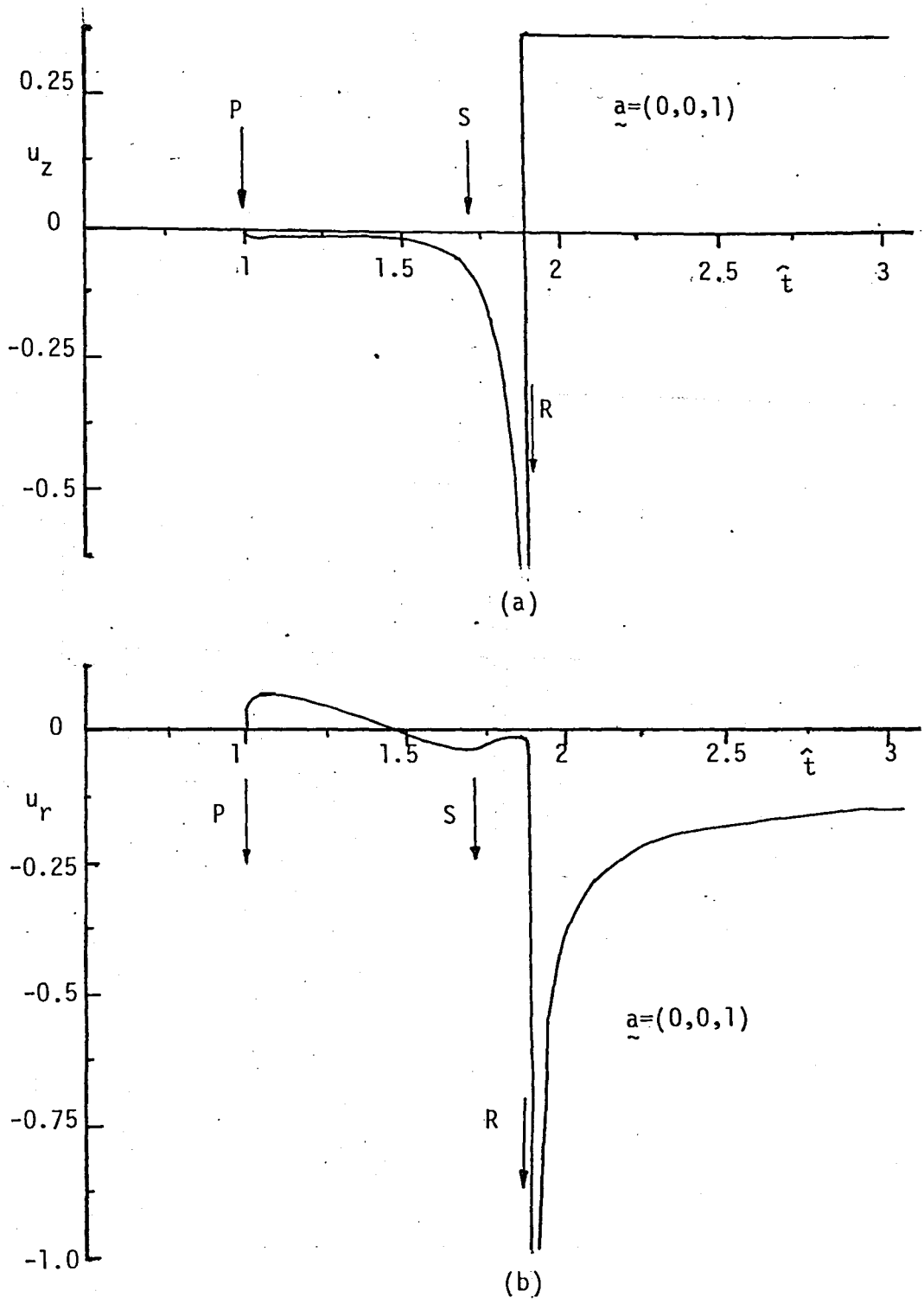
Figure 13. Response due to a surface point source. The ordinate
is the normalized nondimensional displacement
$u = u\pi\mu r_o^2/F_o$ and $\hat{t} = tc/r_o$ with $r_o = 1$ and $z_o = 0$.
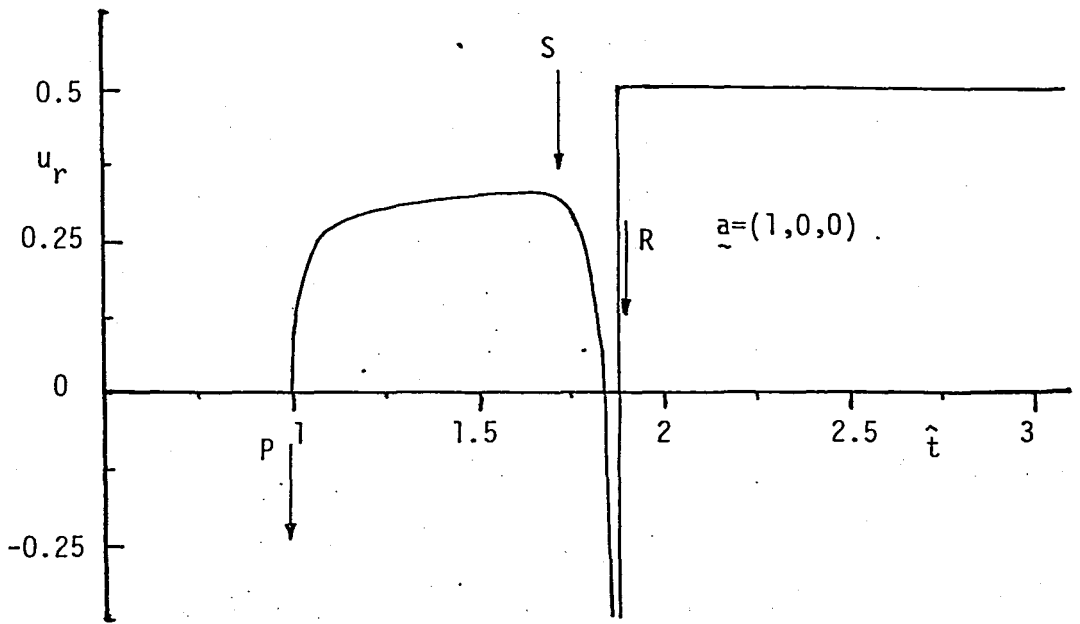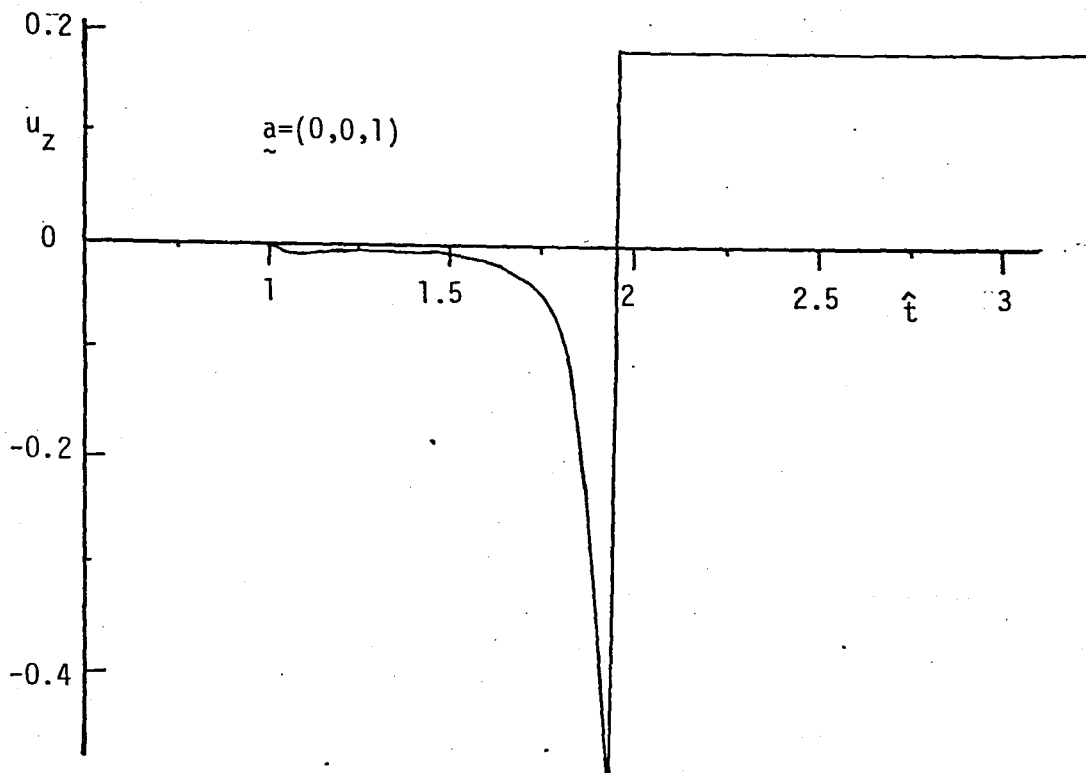
Figure 13c.

Figure 14. Response due to a surface line source, BEH. The ordinate is the normalized nondimensional displacement $u = u\pi\mu r_o^2/F_o$ and $\hat{t} = tc/r_o$ with $r_o = 1$ and $\ell = 0.49$.
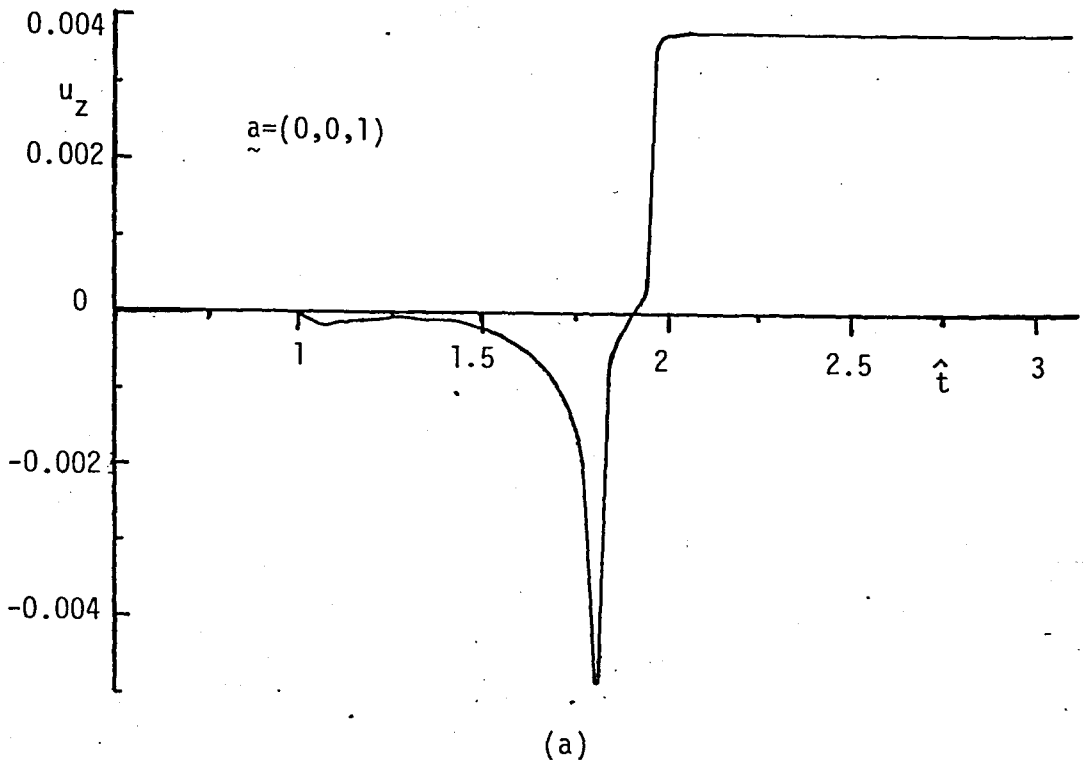
Figure 14c.

Figure 15. Response due to the surface line source, DEF. The
ordinate is the normalized nondimensional displace-
ment $u = u\pi\mu r_o^2 / \dot{F}_o$ and $\hat{t} = tc/r_o$ with $r_o = 1$ and $\ell = 0.49$.
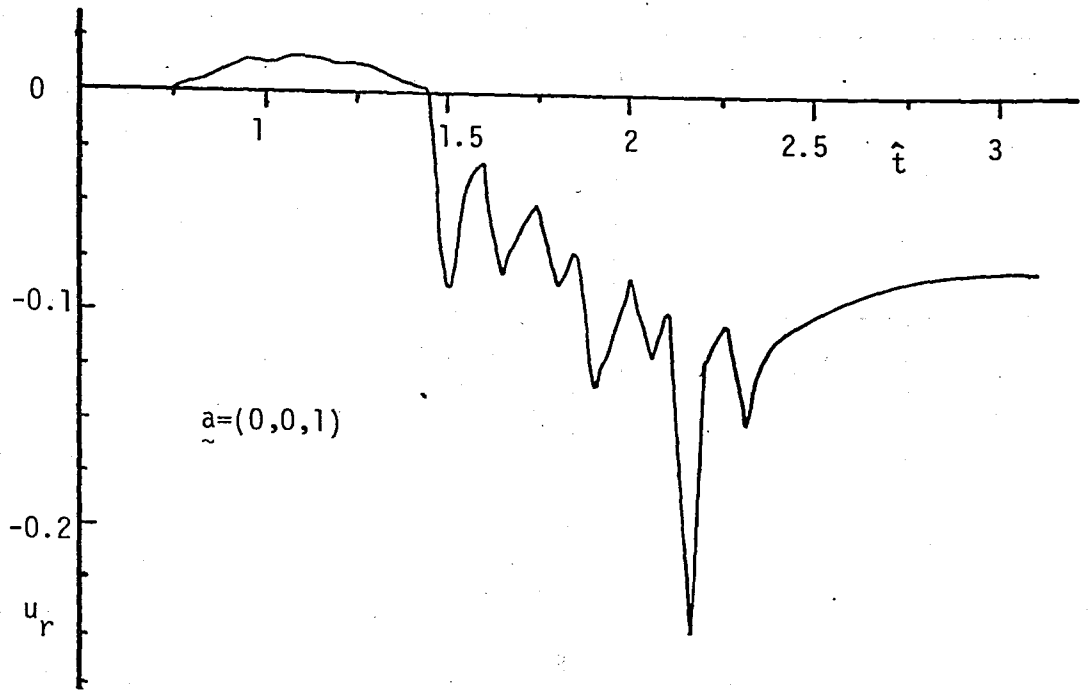
Figure 15b.
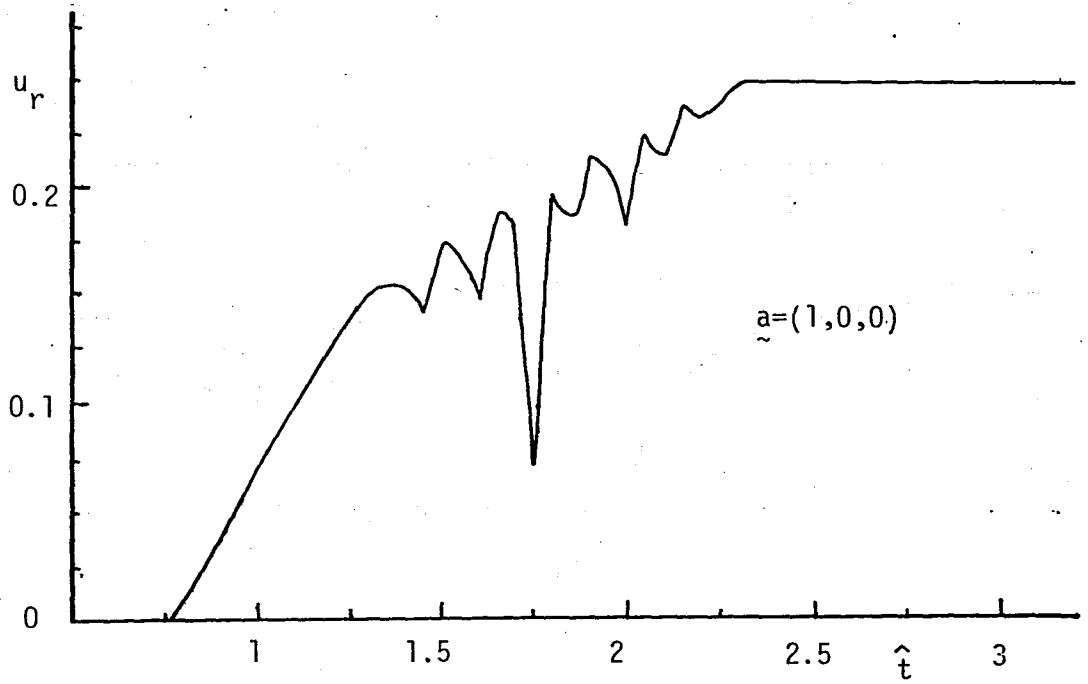
Figure 15c.
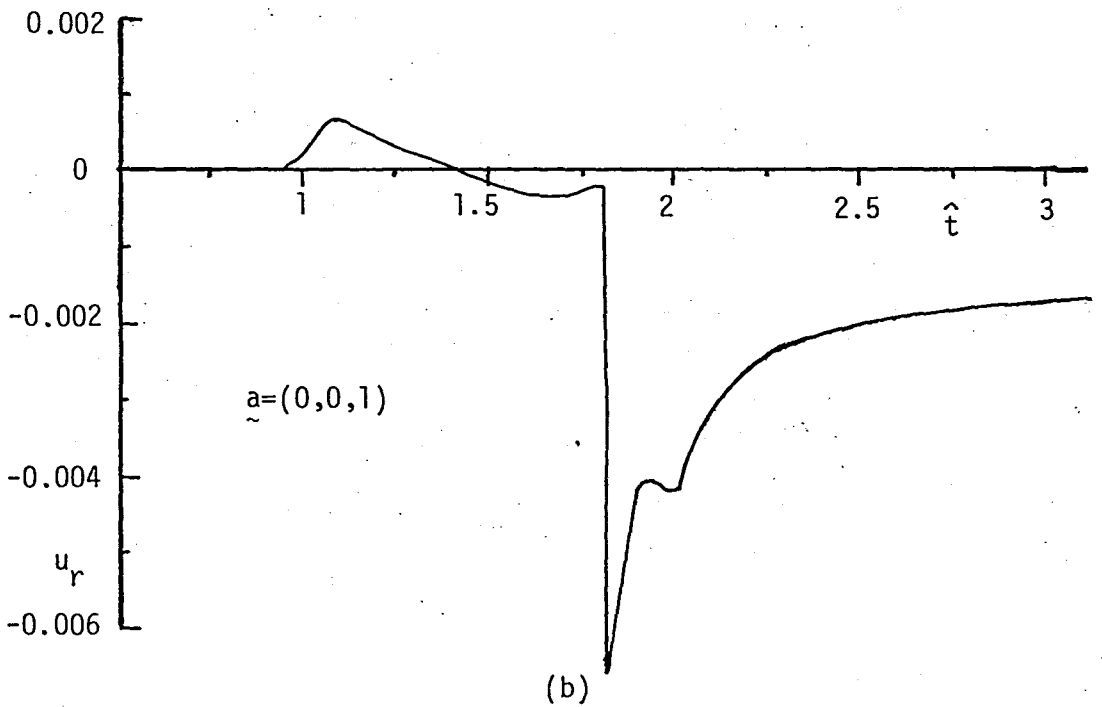
Figure 16. Response due to the surface area source. The ordinate is the normalized nondimensional displacement $u = u \pi \mu r_0^2 / F_0$ and $\hat{t} = tc/r_0$ with $r_0 = 1$ and $\ell = 0.1$.
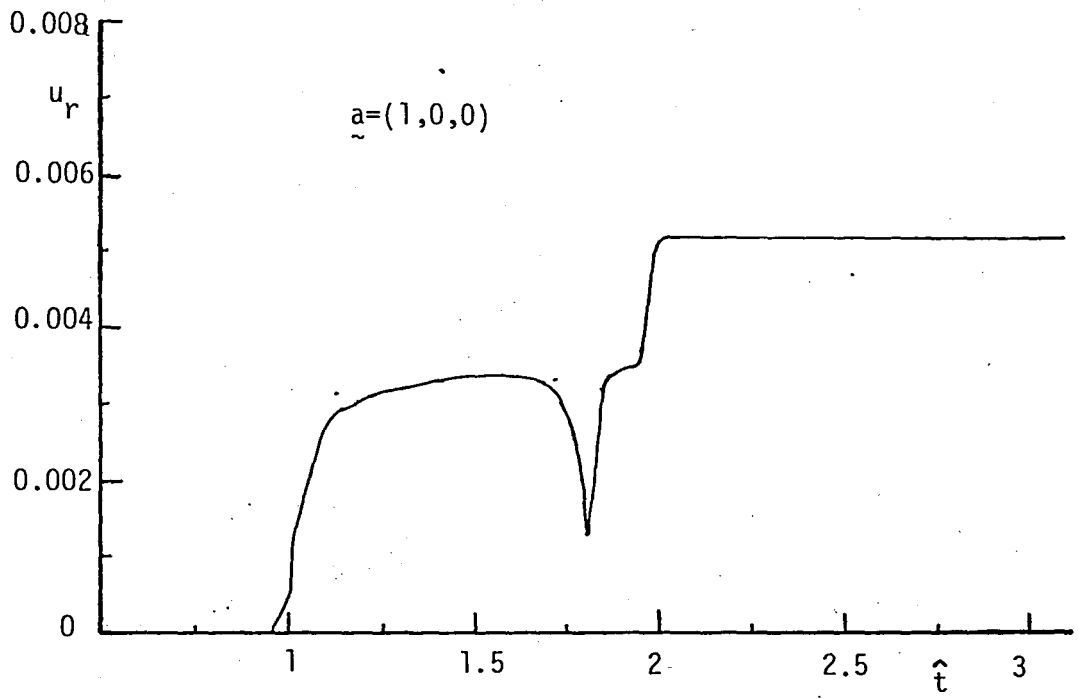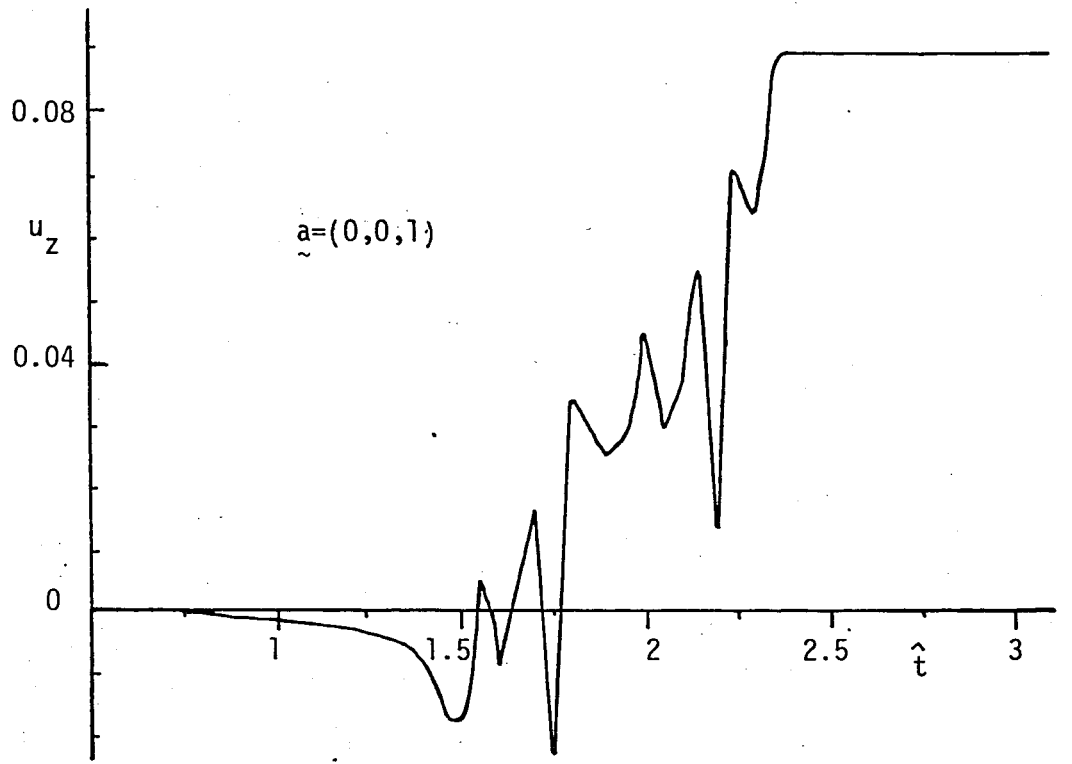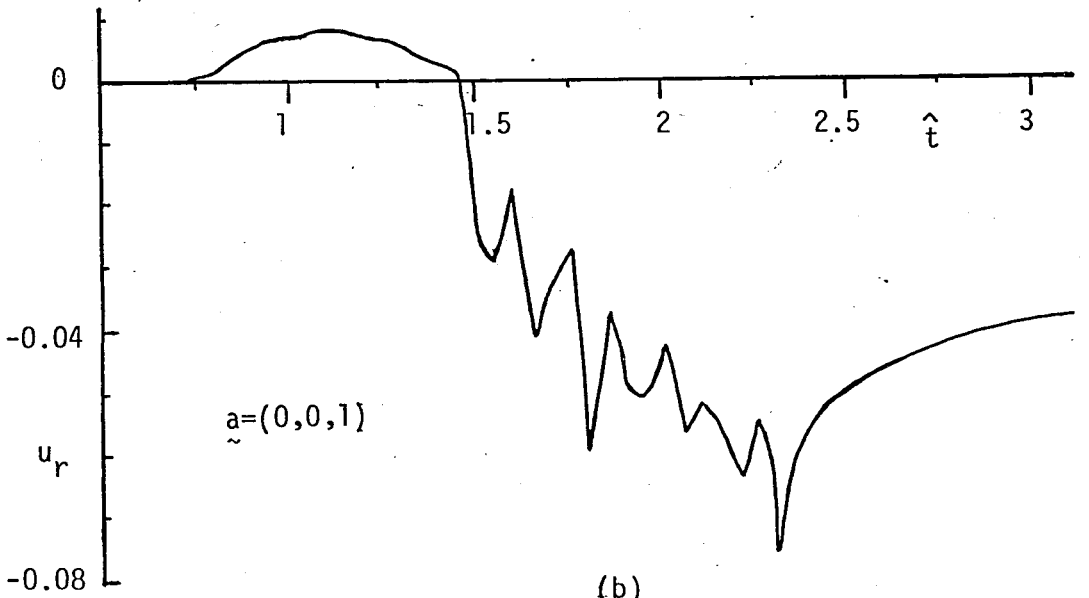
Figure 16c.

Figure 17. Response due to the surface area source. The ordinate is the normalized nondimensional displacement $u = u \pi \mu r_0^2 / F_0$ and $\hat{t} = tc/r_0$ with $r_0 = 1$ and $\ell = 0.49$.
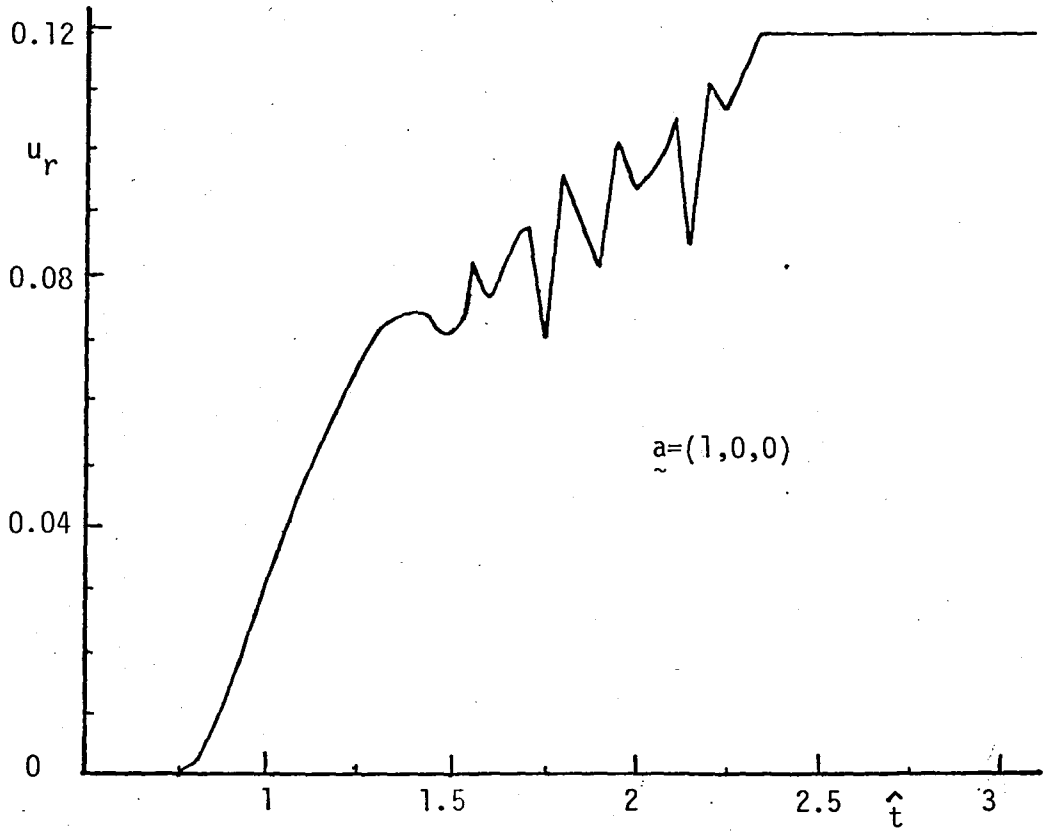
Figure 17c.